

*This paper is a non-peer reviewed preprint submitted to EarthArXiv. The manuscript is a revision submitted to Soil Biology and Biochemistry and currently under peer review. Future updates on this manuscript will be provided once it's peer-reviewed or accepted. Please feel free to contact me at: [arjun.chakrawal@pnnl.gov](mailto:arjun.chakrawal@pnnl.gov) if you have any questions or feedbacks.*

## Highlights

- Bioenergetic assessment of DOM chemodiversity on soil respiration using high-resolution FTICR-MS data.
- High DOM soils showed decreased respiration with increasing alpha diversity; low DOM soils showed increased respiration.
- Chemodiversity-informed kinetics predicting respiration rates did not improve model performance
- Opportunities to advance substrate uptake kinetics by establishing causal links between DOM chemodiversity and microbial metabolism trade-offs

# Challenges in Integrating Dissolved Organic Matter Chemodiversity into Kinetic Models of Soil Respiration

Arjun Chakrawal<sup>1</sup>, Odeta Qafoku<sup>1</sup>, Satish Karra<sup>1</sup>, John R. Bargar<sup>1</sup>, and Emily B. Graham<sup>1,2</sup>

<sup>1</sup>Environmental Molecular Sciences Laboratory (EMSL), Pacific Northwest National Laboratory, PO Box 999, Richland, WA 99352, USA

<sup>2</sup>School of Biological Sciences, Washington State University, Pullman, WA, USA

## Abstract:

The chemodiversity of dissolved organic matter (DOM) in soil has been proposed to influence the microbial metabolism and fate of belowground organic carbon (C). However, effectively integrating DOM chemistry into soil C cycle models to improve predictions of C stocks and fluxes—beyond simply considering DOM pool size—remains a challenge. While recent research suggests that incorporating DOM chemodiversity into models can improve predictions of microbial respiration, there is still a lack of mechanistic understanding describing how DOM chemodiversity affects microbial metabolism and soil respiration. We evaluated whether DOM chemodiversity was a determinant of soil respiration using paired measurements of high-resolution DOM chemistry, obtained from Fourier transform ion cyclotron resonance mass spectrometry (FTICR-MS), and potential soil respiration rates from across the United States (U.S.), all data provided by the Molecular Observation Network. Our objectives were to (1) assess statistical relationships between DOM chemodiversity and microbial respiration, and (2) evaluate the ability of kinetic models to leverage DOM chemistry to explain empirical relationships found in statistical models.

Statistical regressions revealed that DOM chemodiversity (alpha diversity) was nonlinearly related to potential soil respiration rates, both independently and through its interactions with DOM and total C concentrations. In soils with relatively high DOM but low total C concentrations, potential soil respiration rates were negatively correlated with DOM alpha diversity, whereas soils with relatively low DOM and high total C concentrations showed the opposite trend. However, when metabolic transition theory kinetic models were modified to include chemodiversity, their performance was comparable to traditional Monod kinetics approaches, which simulate respiration rates as a function of DOM concentration. The inability to account for non-linearities in DOM chemodiversity–respiration relationships highlight an opportunity to advance substrate uptake kinetics by establishing causal links between DOM chemodiversity, microbial metabolism trade-offs, and interactions under varied environmental conditions.

**Keywords:** FTICR-MS, bioenergetic model, soil organic matter, soil respiration, chemodiversity, carbon cycle modeling

## 1. Introduction

Despite extensive research on the molecular diversity of DOM in soil and aquatic systems (Cui et al., 2024; Hall et al., 2020b; Kalbitz et al., 2003; Tanentzap and Fonvielle, 2024), its implications for microbial metabolism and soil C dynamics remain insufficiently quantified. The transformation and persistence of

DOM in soils result from complex interactions, including microbial decomposition, sorption-desorption dynamics, and abiotic processes (Ding et al., 2020; Kothawala et al., 2021). As DOM undergoes microbial processing, its molecular composition shifts, often leading to a decline in chemodiversity—a potential indicator of soil organic matter degradation status (Davenport et al., 2023; Freeman et al., 2024). However, DOM persistence is influenced by factors other than chemodiversity, such as selective microbial uptake, mineral interactions, and thermodynamic constraints (Boye et al., 2017; Gunina and Kuzyakov, 2021; Lehmann et al., 2020; Mayes et al., 2012; Schmidt et al., 2011). For example, organic acids produced from root exudates can replace mineral-associated C, making it more available for microbial uptake (Keiluweit et al., 2015).

Chemodiversity, which includes characteristics such as molecular weight, degree of aromaticity, and functional group composition, influences the reactivity and bioavailability of DOM (Li et al., 2023; Negassa et al., 2021; Zhou et al., 2021). The chemical nature of these substrates can affect microbial growth efficiency—microorganisms may exhibit high efficiency with compounds like glucose but low efficiency with more recalcitrant substances like oxalate (Chakrawal et al., 2020). This variation in growth efficiency subsequently impacts microbial by-products and necromass production, which play key roles in the in-vivo stabilization of soil organic matter (Manzoni and Cotrufo, 2024). Understanding how the chemodiversity of DOM influences microbial substrate utilization pathways is crucial for improving process representation in models, thereby improving predictions of soil C stocks.

Recent advances in high-resolution mass spectrometry have enabled more precise characterization of DOM molecular diversity (Ayala-Ortiz et al., 2023; Bahureksa et al., 2021). Using various proxies of DOM chemodiversity (indicated by the aromaticity, humification index, the ratio of aromatic to aliphatic C, and the relative abundances of humic-like components), Yang et al. (2024) showed that metabolic quotient decreased with increasing fraction of recalcitrant compounds in DOM. Another study by Shi et al., (2025) demonstrated that integrating DOM chemical signatures (derived via machine learning) improved statistical models of soil respiration (Shi et al., 2025). While such machine learning approaches may enhance predictive accuracy, they do not reveal mechanistic relationships between DOM composition and microbial metabolic pathways. Despite these advances, effectively integrating DOM chemistry into soil C cycle models to improve predictions of C stocks and fluxes—beyond simply DOM pool size—remains a challenge (Graham and Hofmockel, 2022). In this contribution, we aim to investigate how varying degrees of DOM chemodiversity influence soil microbial processes and, consequently, soil C cycling.

Traditional soil C models incorporate the chemical complexity of soil organic matter through operationally defined pools representing varying degrees of soil organic matter physicochemical recalcitrance, characterized using linear kinetic parameters (Parton et al., 1994). More recent models have improved upon this abstraction by conceptually dividing soil organic matter into plant-derived, mineral-associated, dissolved, and/or microbial C pools (Abramoff et al., 2018; Robertson et al., 2019; Wang et al., 2013; Wieder et al., 2014). Despite numerous studies highlighting the chemodiversity of organic compounds found in particulate organic matter (Witzgall et al., 2021), mineral-associated organic matter (Anderson et al., 2023; Lv et al., 2020) and DOM (Ayala-Ortiz et al., 2023; Bahureksa et al., 2021),

even newer models consider these pools to be chemically homogeneous and define their decomposition rates using fixed kinetic parameters. Furthermore, models representing DOM pool metabolism typically use bulk chemistry (i.e., DOM concentration) and fixed kinetic parameters to define the rate of microbial utilization that is not representative of the chemodiversity found in DOM (Camino-Serrano et al., 2018; Yu et al., 2020). Such simplification overlooks the microbially induced transformations of organic matter, and the intricate interactions between microbial uptake, release, and sorption of DOM on mineral reactive surfaces (Amenabar et al., 2017; Keiluweit et al., 2015; Marschmann et al., 2024; Sokol et al., 2019). These processes ultimately dictate the chemical diversity and microbial metabolism and kinetics of DOM. For example, not all mineral surfaces have same sorption capacity for different organic compounds in DOM pools (Mayes et al., 2012). Consequently, microorganisms feeding on these substrates will vary in growth rate and efficiency (Chakrawal et al., 2020).

Recent advancements have highlighted the potential of integrating the chemodiversity of DOM into C cycling models using bioenergetics to predict uptake and microbial growth rates (Chakrawal et al., 2022; Desmond-Le Quémener and Bouchez, 2014; Song et al., 2020). These approaches only account for the average thermodynamic properties of DOM, despite the fact that different chemical classes of DOM have varying bioavailability and thermodynamic properties (Ahamed et al., 2023; Song et al., 2020). Overall, the integration of high-resolution FTICR-MS data into models is still new in the field of modeling soil biogeochemical processes, with considerable uncertainty regarding how effectively these new data-model integration approaches can capture the complexity of DOM chemodiversity and its impacts on ecosystem processes. Despite a strong theoretical basis, these model formulations have yet to be widely tested with empirical datasets.

The present study was designed to address this gap. Our main hypothesis is that DOM chemodiversity is a crucial driver of soil respiration; therefore, incorporating chemical diversity into kinetic parameters will improve model predictions of soil respiration relative to models based on DOM concentration alone. To evaluate our hypothesis, we: (1) assessed the statistical relationships between the chemodiversity of DOM and soil respiration across the continental United States and (2) determined if chemodiversity-informed reaction kinetics improve predictions of soil respiration. Our goal is to identify potential interactions between DOM chemodiversity and edaphic factors and challenge current-generation models to include DOM-chemistry-explicit kinetics for better soil respiration predictions. We use linear regression and random forest analysis to evaluate the potential of various DOM chemodiversity metrics and common soil biogeochemical variables to predict respiration rates. Then, we assess three types of kinetics-based model simulations: Monod kinetics, a single homogeneous DOM pool model, and a multi-pool model. Monod kinetics formulates respiration as a function of DOM concentration only, while the single homogeneous DOM pool model and the multi-pool model are based on metabolic transition state theory, linking soil respiration rates to microbial functional traits derived from DOM chemical properties.

## **2. Methods and Materials**

### **2.1. Data**

We used standardized data collected by the 1000 Soil Pilot program of the Molecular Observation Network (MONet) from topsoil (0-10 cm) in 63 cores across the continental U.S. (CONUS)

(supplementary Figure 1A). MONet data include soil respiration rates, water-extractable OM concentration and chemistry, and over twenty additional biogeochemical parameters. Details of the data types and methodologies regarding data collection from MONet are provided at <https://www.emsl.pnnl.gov/monet#data>, and the data used in this publication—from the MONet Pilot Project, the 1000 Soils Pilot—can be downloaded from (Bowman et al., 2024).

Soil respiration rate was measured using the CO<sub>2</sub> burst method with 24 hours of incubation at 24 °C. The short incubation duration ensured that CO<sub>2</sub> production is primarily due to microorganisms metabolizing easily available organic substrates, with limited impact from other factors such as desorption or priming. This measurement represents the potential respiration rate rather than the actual in situ rate, as the CO<sub>2</sub> burst method stimulates microbial activity through rewetting and incubation, often leading to an overestimation of field respiration rates (McGowen et al., 2018). For brevity, we refer to potential respiration rate simply as respiration rate. DOM chemistry was analyzed with a Bruker 7-T Fourier-transform ion cyclotron resonance mass spectrometry (FTICR-MS). For detailed methodologies regarding data collection, readers are referred to Bowman et al. (2023) and Shi et al. (2025), including their supplementary information.

This study did not collect any new data but rather performed statistical analysis on pre-existing MONet data. As described in Shi et al. (2025), FTICR-MS detected over 7,000 unique DOM molecules, which were then assigned chemical formulas using CoreMS. We used Van Krevelen analysis to categorize these molecules into nine broad molecular classes: Amino Sugar-like, Carbohydrate-like, Condensed Hydrocarbon-like, Lignin-like, Lipid-like, Protein-like, Tannin-like, Unsaturated Hydrocarbon-like, and Other. Van Krevelen analysis assigns an organic compound to a class if its H:C and O:C ratios fall within the specified upper and lower limits for that class (Ayala-Ortiz et al., 2023; Bahureksa et al., 2021; Bailey et al., 2017). These chemical classes represent class-like categories because they rely on elemental composition and do not capture structural complexity (e.g., lignin-like or carbohydrate-like). Nonetheless, FTICR-MS offers unmatched resolution in DOM composition, enabling the detection of a wide range of DOM compounds using available analytical techniques.

## 2.2. Microbial growth reaction and growth kinetics

To account for the chemical diversity and concentration of DOM while estimating soil respiration rate, we used a bioenergetic approach that integrates the thermodynamic properties of different organic compounds as parameters in kinetic models. We applied the bioenergetic framework described by Song et al. (2020) and employed by Ahamed et al. (2023) and Zheng et al. (2024) to formulate a metabolic reaction network describing the metabolic growth reaction of microorganisms under aerobic conditions, specific to each chemical class in each soil sample.

By representing the chemical formula of a generic organic compound as C<sub>a</sub>H<sub>b</sub>N<sub>c</sub>O<sub>d</sub>P<sub>e</sub>S<sub>f</sub><sup>Z</sup> and microbial biomass as CH<sub>1.8</sub>N<sub>0.2</sub>O<sub>0.5</sub>, the growth reaction is expressed as follows,



where, *a*, *b*, *c*, *d*, *e* and *f* are average number of atoms of the respective element from all compounds assigned a specified chemical class, *y*<sub>OC</sub>, *y*<sub>O<sub>2</sub></sub>, and *y*<sub>CO<sub>2</sub></sub> are the stoichiometric coefficients of organic

compound, oxygen, and CO<sub>2</sub>, respectively. Note that even though chemical classes are broadly defined into nine categories, their chemical formula can vary across soil samples, resulting in different stoichiometric coefficients for each chemical class and soil sample. The stoichiometric coefficients in the metabolic reaction are calculated using the thermodynamic favorability factor  $\lambda$  defined as the ratio of the sum of change in Gibbs energy dissipated and conserved in biomass to the Gibbs energy generated from catabolism, as follows,

$$\lambda_{i,j} = \frac{\Delta G_{diss,i,j} + \Delta G_{an,i,j}}{-\Delta G_{cat,i,j}}, \quad (2)$$

where the subscripts  $i$  and  $j$  represents the microbial growth reaction for  $i^{th}$  chemical class in  $j^{th}$  soil sample.  $\Delta G_{diss,i,j}$ ,  $\Delta G_{an,i,j}$ , and  $\Delta G_{cat,i,j}$  are the change in Gibbs energy metabolic, anabolic, and catabolic reactions. A higher value of  $\lambda_{i,j}$  denotes less favorable organic compound because catabolism needs to run a greater number of times to produce 1C mol of biomass, requiring more energy to be generated from catabolism. For details in calculating the change in Gibbs energy values for catabolic and anabolic reaction, reader are referred to (Chakrawal et al., 2022; Kleerebezem and Van Loosdrecht, 2010; LaRowe and Van Cappellen, 2011; Song et al., 2020). The changes in Gibbs energy were corrected for observed pH in soil pore water (Amend and LaRowe, 2019; Song et al., 2020).

The stoichiometric coefficients of organic compound and CO<sub>2</sub> can now be calculated as a function of  $\lambda$  as follows,

$$y_{OC,i,j} = \lambda_i + y_{OC,i,j}^{an}, \quad (3)$$

$$y_{CO_2,i,j} = y_{OC,i,j} a_{i,j} - 1, \quad (4)$$

where  $y_{OC,i,j}^{an}$  is the stoichiometric coefficient of organic compound in the anabolic reaction and  $a_{i,j}$  is the number of C atoms in the chemical formula of organic compound.

We used the metabolic transition state theory (MTS) (Desmond-Le Quéméner and Bouchez, 2014) to calculate the rate of the microbial growth (which is equivalent to the reaction rate in eq 1) as a function of the stoichiometric coefficients ( $y_{OC,i,j}$  and  $y_{CO_2,i,j}$ ) and DOM concentration ( $S_{DOM,i,j}$ ). The microbial growth rate is expressed as follow,

$$\mu_{i,j} = N \mu_{i,j}^{max} \exp\left(-\frac{y_{OC,i,j}}{V_h S_{DOM,i,j}}\right), \quad (5)$$

where  $\mu_{i,j}$  represents the microbial growth rate for  $i^{th}$  chemical class in  $j^{th}$  soil sample,  $\mu_{max,i,j}$  is the maximum growth rate,  $V_h$  is the volume harvest parameter representing accessible volume by microorganisms to acquire chemical energy from their surroundings (Ugalde-Salas et al., 2020), and  $N$  is a normalization factor used to express growth rate in the units of mgC g<sup>-1</sup> soil day<sup>-1</sup>. From the microbial growth rate, the substrate uptake rate can be calculated as  $q_{i,j} = a_{i,j} y_{OC,i,j} \mu_{i,j}$ , C use efficiency (CUE) to be defined as the ratio of the growth rate to the substrate uptake rate, yielding the expression  $CUE_{i,j} = \frac{1}{a_{i,j} y_{OC,i,j}}$ . This represents the maximum CUE attainable under no nutrient limited conditions (Chakrawal

et al., 2022). The respiration rate can be obtained by multiplying  $\mu_{i,j}$  by the stoichiometric coefficient of  $\text{CO}_2$ , yielding  $R_{i,j} = y_{\text{CO}_2,i,j} \mu_{i,j}$ .

To estimate  $\mu_{\text{max},i,j}$ , we first calculated the maximum substrate uptake rate ( $q_{\text{max},i,j}$ ) as a function of number of electrons ( $N_e$ ) transferred from organic C to electron acceptor during catabolism, following González-Cabaleiro et al. (2015). The equations for  $q_{\text{max},i,j}$  and  $\mu_{\text{max},i,j}$  are as follows,

$$q_{\text{max},i,j} = \frac{3}{N_e} \quad (6)$$

$$\mu_{\text{max},i,j} = \text{CUE}_{i,j} q_{\text{max},i,j} \quad (7)$$

### 2.3. Chemodiversity-informed microbial growth kinetics

Using MTS kinetics, we formulated two chemodiversity-informed microbial growth kinetics models: a single homogeneous DOM pool model and a multi-pool model. In the homogeneous DOM pool model, we define a single pool of DOM by the average thermodynamic properties of the DOM. Using average values of  $y_{\text{OC},i,j}$  and  $y_{\text{CO}_2,i,j}$  across chemical classes, and concentration of DOM from each soil sample, the soil respiration rate,  $R_{\text{MTS}}^{\text{mean}}$  from the single pool model is calculated as,

$$R_{\text{MTS}}^{\text{mean}} = N \bar{\mu}_{\text{max},j} \overline{y_{\text{CO}_2,j}} \exp\left(-\frac{\overline{y_{\text{OC},j}}}{V_h S_{\text{DOM},j}}\right) \quad (8)$$

In eq. 8, while the model parameters are averaged across nine chemical classes (dropping the class subscript,  $i$ ), they continue to vary by soil sample (retaining the sample subscript  $j$ ). The overline symbols represent average statistics.

In the multi pool model, we calculated soil respiration ( $R_{\text{MTS}}^{\text{multi}}$ ) as the sum of respiration from all chemical classes of DOM, considering the variation in their concentration and model parameters  $y_{\text{OC},i,j}$ ,  $y_{\text{CO}_2,i,j}$ , and  $\mu_{\text{max},i,j}$  values for each chemical class. The concentration of DOM ( $S_{\text{DOM},i,j}$ ) in each chemical class was estimated by multiplying the total DOM concentration by the relative proportion of peaks within that class (expressed as a percentage of total peaks). The respiration rate for a multi-pool model is given as,

$$R_{\text{MTS}}^{\text{multi}} = N \sum_{i=1}^9 y_{\text{CO}_2,i,j} \mu_{\text{max},i,j} \exp\left(-\frac{y_{\text{OC},i,j}}{V_h S_{\text{DOM},i,j}}\right) \quad (9)$$

We also considered Monod kinetics with a single pool DOM as a reference model where model parameters were directly fitted using observed respiration (Table 1). Parameters  $V_h$  and normalization factor  $N$  in MTS, and the maximum respiration rate ( $V_{\text{max}}$ ) and half saturation ( $K_m$ ) in Monod kinetics were estimated as best fitted parameters by fitting the model to observed rates of soil respiration. Parameter values, model performance indices, the coefficient of determination ( $R^2$ ), and root mean squared error (rmse) are provided in Table 1.

Table 1 Kinetic rate expression for soil respiration as a function of stoichiometric coefficients of DOM ( $y_{OC}$ ) and  $CO_2$  ( $y_{CO_2}$ ), and DOM concentration ( $S_{DOM}$ ) for three kinetic formulations. Estimated model parameters and model performance indices (coefficient of determination ( $R^2$ ) and root mean squared error (rmse) is also included.

| Model             | Rate expression  | Maximum rate constant ( $V_{max}$ in $day^{-1}$ ) or Normalization constant ( $N$ , in $mg\ C\ g^{-1}\ soil$ ) | Half saturation constant ( $K_M$ in $mg\ C\ g^{-1}\ soil$ ) or volume harvest parameter ( $V_h$ in $(mg\ C\ g^{-1}\ soil)^{-1}$ ) | $R^2$ [-] | rmse [ $mg\ C-CO_2\ g^{-1}\ soil\ day^{-1}$ ] |
|-------------------|--|--|---|-----------|---|
| Monod             | $R_{Monod} = \frac{V_{max}S_{DOM}}{S_{DOM} + K_m}$   | $V_{max} = 1.58$   | $K_M = 0.935$   | 0.55      | 0.123   |
| MTS (Single pool) | $R_{MTS}^{mean} = N \bar{\mu}_{max_j} \overline{y_{CO_2,j}} \exp\left(-\frac{\overline{y_{OC,j}}}{V_h S_{DOM,j}}\right)$ | $N = 1.8$  | $V_h = 0.57$  | 0.57      | 0.120   |
| MTS (Multi pool)  | $R_{MTS}^{multi} = N \sum_{i=1}^9 y_{CO_2,i,j} \mu_{max,i,j} \exp\left(-\frac{y_{OC,i,j}}{V_h S_{DOM,i,j}}\right)$       | $N = 0.84$   | $V_h = 1.42$  | 0.56      | 0.121   |

#### 2.4. Statistical analysis of soil respiration.

We used linear regression and random forest models to predict soil respiration as a function of DOM chemodiversity and biogeochemical variables. DOM chemodiversity related variables were calculated from FTICR-MS data. To represent the chemical nature of DOM in a soil sample, we used the average chemical properties, nominal oxidation state of C (NOSC), double bond equivalent, molecular weight of DOM, and thermodynamic favorability factor,  $\lambda$  (eq 2), and mean molecular weight of DOM (supplementary Figure S1). Further, to represent chemodiversity of DOM in a soil sample, we used alpha diversity defined here as the number of detected organic compounds (Danczak et al., 2023), Shannon diversity index, coefficient of variation in  $\lambda$  and CUE (supplementary Figure S2). For model selection, we first removed predictors with an insignificant correlation with respiration using  $p$ -value > 0.05 threshold in Pearson correlation coefficient. Subsequently, we removed multicollinear predictors with Pearson correlation coefficients of more than 0.6 (see supplementary Figures S3, S4 and S5).

In our preliminary model, we included soil moisture content, clay content (%), DOM concentration, CN ratio of water-extractable C and N (organic and inorganic), total C (%), pH, and alpha diversity as predictors. To enhance interpretability, respiration was log10-transformed, and all predictors were

centered and scaled. We started with a linear mixed effect model using biome type a random effect on intercept; however, later, it was dropped due to the high Akaike information criterion (AIC) compared to the linear model as a base model. We selected the best-fit linear regression following a sequential model selection approach, beginning with the most complex model (including all interaction terms) and simplifying the model based on the Akaike information criterion and log-likelihood test (see supplementary Table S1). We also used a random forest (RF) regression model to rank importance of predictors where all data points were used for training. Linear regression was performed using R statistical software (R Core Team, 2023), version 4.3.2 and for summarizing regression results in tabular format, the modelsummary package (Arel-Bundock, 2022) was employed. For RF, we used randomForest package in R, and predictors and respiration rate were used in original scale.

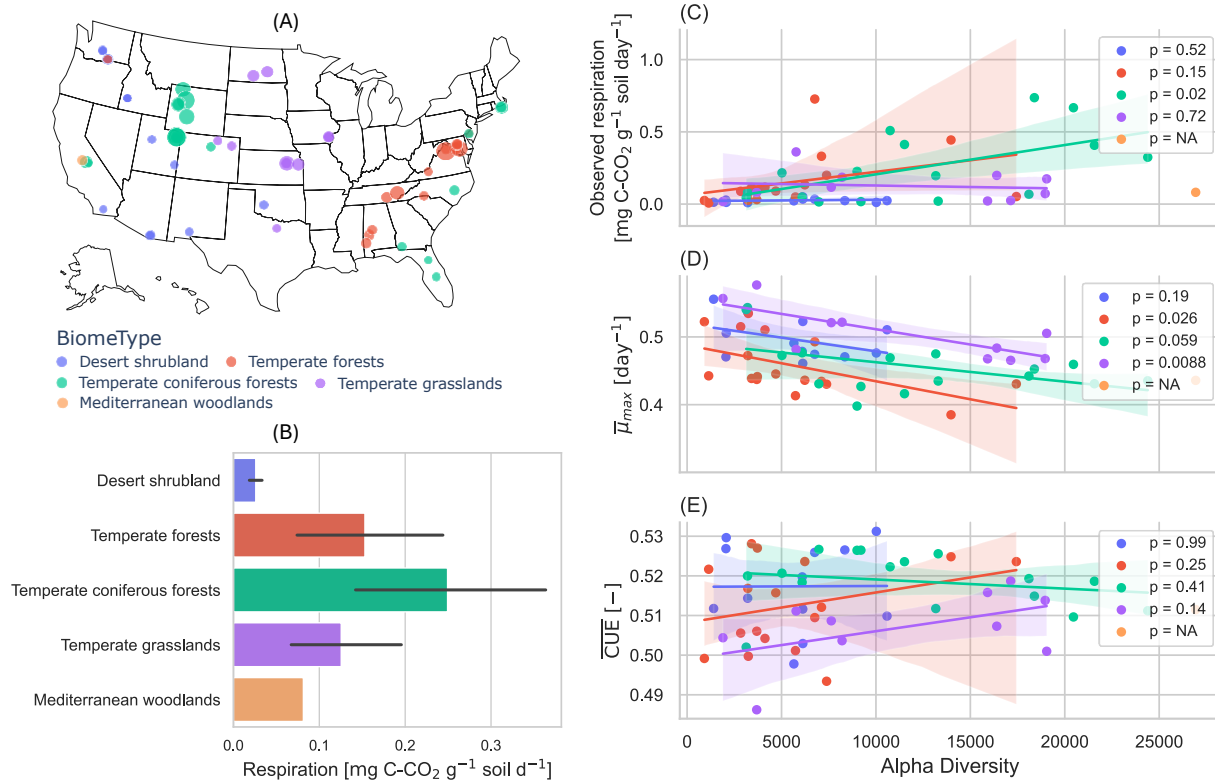


Figure 1 (A) Location of collected soil cores with colors and size of circles illustrating biome type and soil respiration rate, respectively, and (B) Variation of respiration rate across biome types. Variation of (C) observed respiration and estimated microbial functional traits (D) maximum growth rate ( $\bar{\mu}_{max}$ ) and (E) C use efficiency ( $\overline{CUE}$ ) with alpha diversity across different biomes. Note that overbar in maximum growth rate and C use efficiency represents average properties across the chemical classes. Univariate regression lines are fitted to the data points to illustrate trends across different biome types and the p-values are indicated in the legends.

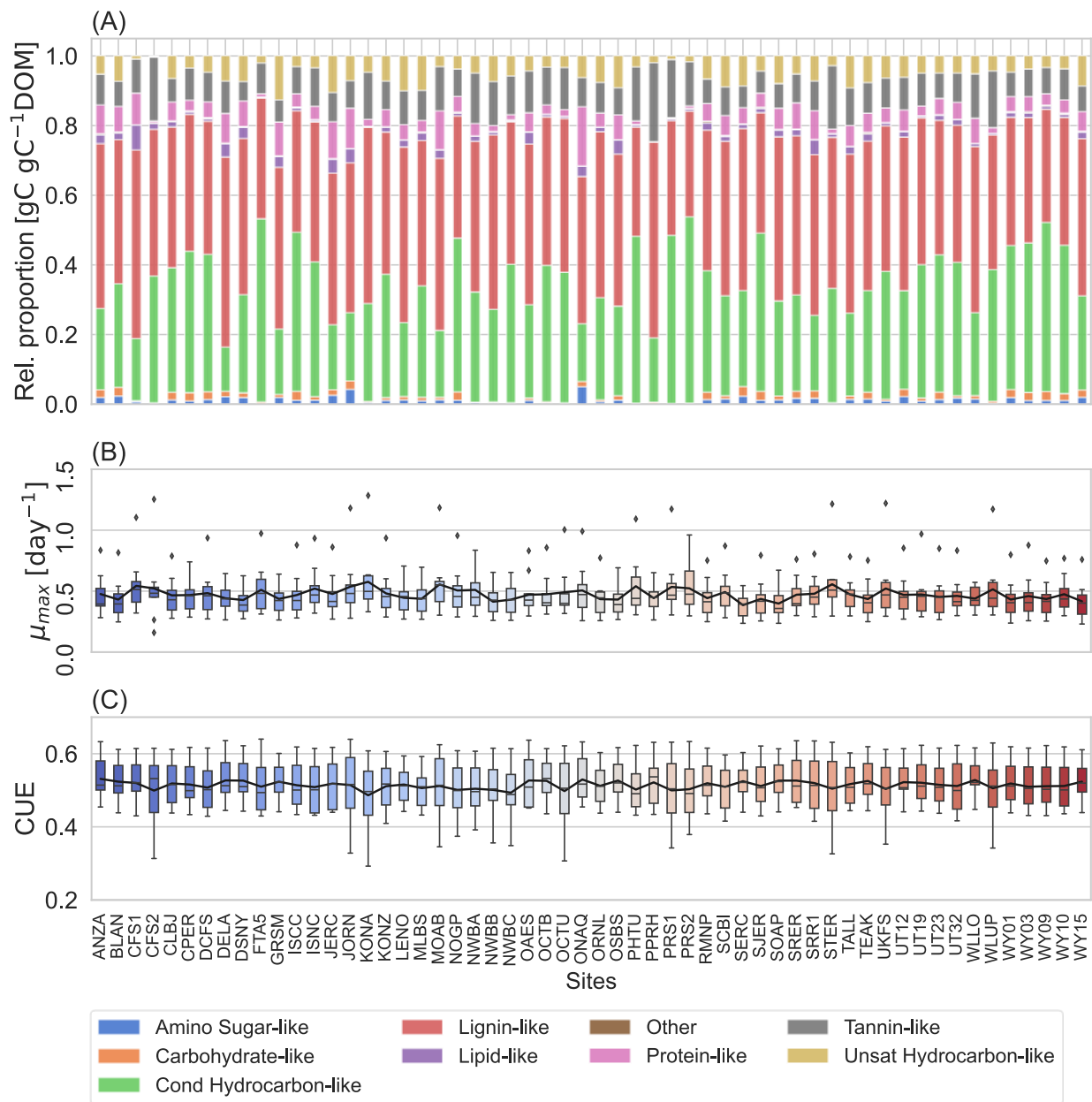


Figure 2 Relative proportion of chemical classes and microbial functional traits ( $\mu_{max}$  and CUE) across soil samples. Boxplots of (A) stacked bar chart showing relative proportion of each class of dissolved organic matter (in gC g<sup>-1</sup>C DOM) (B) maximum growth rate ( $\mu_{max}$ ), and (C) C use efficiency (CUE). The box boundaries represent the 25th and 75th quantiles, with the central line indicating the median. Whiskers extend to 1.5 times the interquartile range and with diamond symbols as outliers.

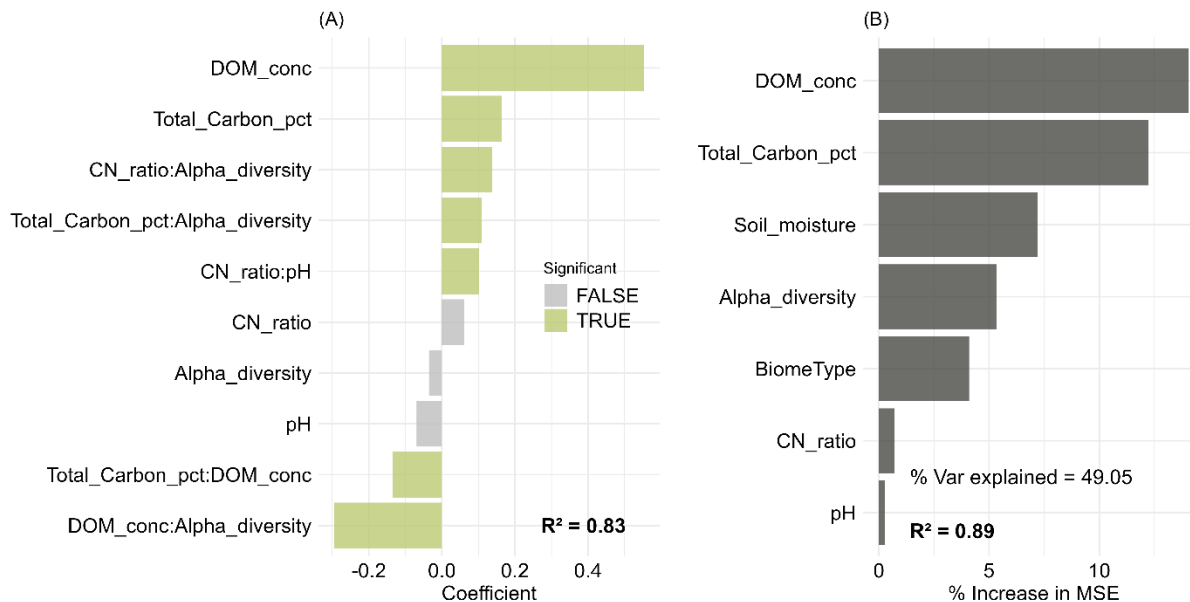


Figure 3 Bar plots of (A) linear regression coefficients and (B) random forest predictor importance for predicting respiration rate. In panel (A), significant predictors are highlighted in green, while insignificant predictors are shown in grey. In panel (B), importance is shown as a percentage increase in mean squared error (MSE) upon feature permutation. The R<sup>2</sup> values indicate coefficient of determination from both models, and %Var explained indicates the proportion of the total variance in respiration rate that is explained by predicted rate from random forest model. Abbreviations: DOM\_conc – dissolved organic matter concentration, Total\_Carbon\_pct – total carbon (%), and CN\_ratio – ratio of DOM concentration to water-extracted total nitrogen.

### 3. Results

#### 3.1. Chemodiversity of DOM across CONUS

Soil respiration rates varied spatially, with temperate coniferous forests showing relatively higher rates compared to other biomes (Figure 1A and 1B). The alpha diversity of DOM varied by more than one order magnitude (range of 914-26933), indicating substantial differences in chemodiversity across soils in CONUS (Figure 1, C-E). Based on univariate analysis, observed respiration generally increased with alpha diversity across biomes (Figure 1C). In contrast, the maximum growth rate decreased (Figure 1D), and CUE showed mixed trends (Figure 1E). All soils displayed high relative proportion of lignin- and condensed hydrocarbon-like DOM peaks compared to other chemical classes, with substantial variation in the proportion of these classes among different soils (Figure 2A). Consequently, CUE, maximum growth rate (Figure 2B and 2C), and stoichiometric coefficients  $y_{OC}$  and  $y_{CO_2}$  in metabolic reactions (Figure S6) varied across compound classes and different soils.

#### 3.2. Is DOM chemodiversity an important variable for explaining soil respiration?

Correlation analysis revealed a significant positive relationship between soil respiration and both alpha diversity and the coefficient of variation of CUE (Figure S1). Additionally, respiration rate was positively correlated with DOM average double bond equivalents and average molecular weight of DOM (Figure

S2); total C, nitrogen, water-extractable C and N concentrations, microbial biomass C and N, and clay content (Figure S3). There was no significant correlation between respiration and the Shannon diversity index, the coefficient of variation of CUE, the average and coefficient of variation of thermodynamic factor of DOM, soil temperature, total C to total N ratio, or microbial C to N ratio.

The linear model identified DOM concentration, total C, alpha diversity, and their interactions as the strongest predictors of respiration, in order of decreasing importance (Figure 3A). This model explained approximately 83% of the observed variability in respiration, with an  $R^2$  of  $0.69 \pm 0.13$  in fivefold cross-validation. The RF model ( $R^2 = 0.89$  and % Variance explained = 49%) identified a similar predictor ranking, with DOM concentration, total C, soil moisture, and alpha diversity as the top four variables (Figure 3B).

The linear model predicted that DOM concentration and total C were positively associated with respiration rate. In soils with relatively high DOM concentrations, respiration rate was negatively correlated with DOM alpha diversity, whereas soils with relatively low DOM concentrations, respiration rate was positively correlated with DOM alpha diversity (red vs. pink lines in Figure 4A). The regression model also detected a positive correlation between respiration rate and the interaction term between total C and alpha diversity (Total\_Carbon\_pct:Alpha\_diversity in Figure 3A), suggesting higher total C increased the positive effect of alpha diversity on respiration (Figure 4B). Additionally, a negative correlation between respiration rate and the interaction term of total C and DOM concentration (Total\_Carbon\_pct:DOM in Figure 3A) indicated that the positive effects of DOM concentration on respiration was reduced when total C increased (Figure 4C). Overall, the regression model indicated that DOM chemodiversity is a significant predictor of soil respiration, along with other predictors such as dissolved OC concentration, total C, and soil moisture. These findings highlight that soil respiration is indeed influenced not only by C availability but also by its chemical diversity.

### 3.3. Comparing DOM chemodiversity-informed kinetic models

The significant statistical correlations between DOM chemodiversity and respiration derived from the regression models suggests that kinetic models can be improved by considering chemodiversity. We tested this conclusion by comparing the performance of chemodiversity-informed kinetic models against a traditional Monod kinetics model. The Monod kinetics model, which simulates respiration rate as a function of DOM concentration, predicted soil respiration rates with an  $R^2$  of approximately 0.55 (Figure 5). When thermodynamic properties of DOM were incorporated with single pool (average  $\mu_{max}$  and stoichiometric coefficients  $y_{OC}$  and  $y_{CO_2}$ ) or a multi pool (varying  $\mu_{max}$ ,  $y_{OC}$ , and  $y_{CO_2}$  for discrete chemical classes), the performance of the MTS kinetics model was similar to that of the Monod model ( $R^2 = 0.55$  and  $0.56$ , respectively, Figure 5 and Table 1). These findings suggest that chemodiversity-informed kinetic models were not substantial improvements over the Monod model. Overall, all kinetic models, including the chemodiversity-informed models predicted soil respiration rates less accurately than the regression models ( $R^2 \approx 0.55$  for kinetics model vs.  $R^2 \approx 0.83$  for regression-based models). Thus, we conclude that these kinetic models do not fully capture the relationship between chemodiversity and C availability. Potential reasons for this behavior and further improvements to better integrate chemodiversity into kinetic models are discussed in section 4.2.

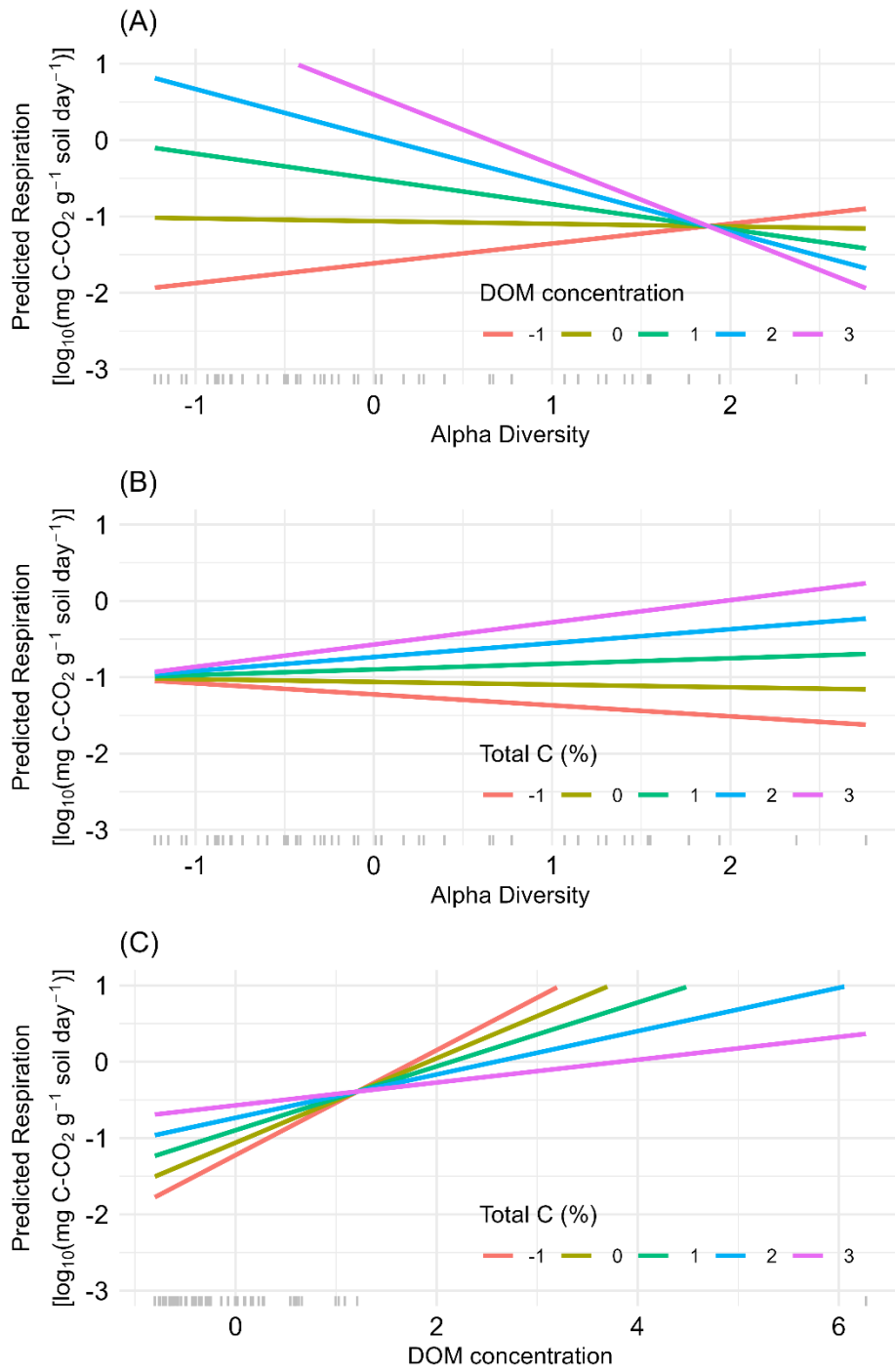


Figure 4 Interaction plot from the linear regression model showing the variation of soil respiration with alpha diversity for varying concentrations of dissolved organic matter (DOM) in (A), and total C in (B). The panel C shows soil respiration as a function of DOM concentration for varying values of total C %. The

respiration rate is in the log10 transformed scale, while DOM concentration, total C % and alpha diversity are on a standardized scale with a mean of zero and a standard deviation of one. A rugplot is included along the x-axis to depict the distribution of the data points.

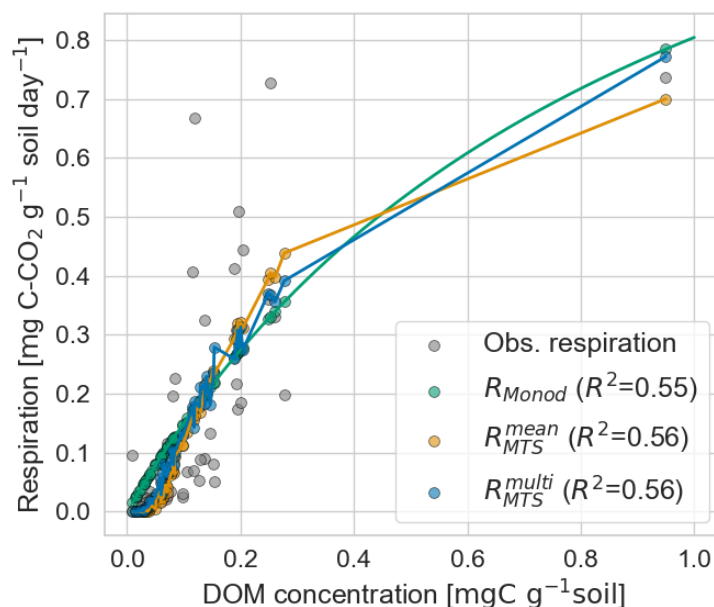


Figure 5 Observed and simulated soil respiration as a function of dissolved organic matter (DOM) concentration. Observed (grey) and modeled soil respiration rates using Monod kinetic  $R_{Monod}$  (green) and metabolic transition state kinetics,  $R_{MTS}^{mean}$  (single pool, yellow) and  $R_{MTS}^{multi}$  (multi pool, blue).

## 4. Discussion

### 4.1. Variability in DOM chemodiversity across CONUS

The high relative proportions of lignin- and condensed hydrocarbon-like DOM compared to other chemical classes (Figure 2) are consistent with the findings of other studies (Li et al., 2019; Yang et al., 2024), which have reported the dominance of recalcitrant compounds such as lignin and tannins in soil-derived DOM. However, the substantial variation observed in the proportions of these compounds among soils highlights the influence of local factors, including vegetation type, soil texture, and the extent of microbial processing (Davenport et al., 2023).

The persistence of lignin- and tannin-like compounds (with aromatic functional groups) is not necessarily due to chemical recalcitrance, as several studies have shown faster decay of lignin compared to bulk SOC (Hall et al., 2020a; Thevenot et al., 2010). This persistence is primarily because the degradation of these compounds requires specialized oxidative enzymes (Mattila et al., 2022). The synthesis of these oxidative enzymes is energetically costly, especially when microorganisms lack labile substrates to fuel their

metabolism (del Cerro et al., 2021; Kirk and Farrell, 1987). Consequently, lower proportions of easily metabolizable compounds such as carbohydrate-, protein-, and amino-sugar-like molecules in DOM may indicate insufficient resource investment to produce oxidative enzymes (Chakrawal et al., 2024; Dao et al., 2022). This could explain the persistence of lignin- and condensed hydrocarbon-like compounds across all soils.

#### **4.2. Correlations of respiration with DOM chemodiversity depend on C availability**

The relationship between DOM chemodiversity and soil respiration rates is influenced by the ability of microorganisms to produce enzymes to break down complex organic matter, which in turn depends on the availability of C in the soil (Sinsabaugh et al., 2009). Lehmann et al (2020) suggested that microbial communities adapted to environments with lower DOM chemical diversity may not produce a wide range of enzymes due to the associated cost of enzyme production (Nunan et al., 2020; Scott et al., 2010). This implies that higher alpha diversity of DOM could lead to reduced overall decomposition potential in some cases and, thus, lower net respiration rates. Our linear regression analysis supports with this hypothesis, revealing a decrease in respiration rate with increasing DOM alpha diversity in soils with high DOM concentrations (Figure 4A, DOM>0). Interestingly, we also found a negative relation between  $\mu_{max}$  and DOM alpha diversity irrespective of high or low DOM concentration, supporting the postulations of Lehmann et al (2020).

However, an opposite trend (increasing respiration with increasing DOM alpha diversity) was observed for soils with low DOM concentrations (Figure 4A, DOM < 0), suggesting that soil microorganisms in a C limited environment may still produce enzymes at a minimal level of enzymes to meet basal metabolic activities. The negative coefficient for DOM:Total C interaction term found in our regression model (Figure 3A) suggests that microorganisms, when faced with limited readily available C (low DOM concentrations), utilize their metabolic diversity to exploit more complex or less accessible C sources present in the soil. For soils with high DOM alpha diversity, this capability is likely enhanced (positive Total C:alpha diversity term in Figure 2A) possibly by producing extracellular enzyme action to break down complex compounds, converting them into accessible forms. Consequently, even with low DOM concentrations, the increased alpha diversity may allow for increased microbial activity and enzyme production, thereby increasing respiration rates. Furthermore, higher DOM alpha diversity at low DOM concentrations has been associated with new niche spaces for complementary organisms that may also enhance respiration rates at the community level (D'Andrilli et al., 2019; Logue et al., 2016; Wang et al., 2022).

While the regression analysis may not establish cause-effect relationships, it suggests that DOM chemodiversity may drive shifts in microbial metabolism, which can be interpreted through the lens of the Yield-Acquisition-Stress (YAS) trait-based paradigm (Malik et al., 2020). Although we did not find a direct significant relationship between alpha diversity and CUE, higher alpha diversity was associated with an increased proportion of putative labile compounds and consequently higher CUE (Figure S7). This suggests that under high C availability, increasing DOM alpha diversity may promote the dominance of Y-strategist microbial communities, adapted for maximizing CUE and biosynthesis. Conversely, under low resource conditions, it may favor A-strategist communities, investing more in extracellular enzymes

to access a broader range of substrates. These findings can be used for generating hypotheses about how DOM chemodiversity may be associated with soil microbial activity, such as increased investment in enzymes, growth, or respiration. For instance, testing how varying degrees of DOM chemodiversity, by introducing different types of labile organic compounds under varying DOM concentrations, influences microbial metabolic trade-offs can help us understand whether DOM chemodiversity-controlled trade-offs in microbial metabolism can lead to either a loss of C through respiration or SOM buildup through increased microbial growth in the long term. We anticipate that such empirical investigations will be critical for informing microbial-explicit models by linking DOM chemodiversity to microbial functional traits and metabolism-driven trade-offs.

#### **4.3. DOM chemodiversity-informed kinetic models failed to improve soil respiration prediction**

Regression analysis elucidated that alpha diversity influenced respiration rate differently under high and low DOM concentration conditions, supporting our hypothesis that incorporating the chemical diversity of DOM enhances predictions of soil respiration. However, incorporating variability in DOM chemistry, as encoded in MTS model parameters ( $\mu_{max}$ ,  $y_{OC}$ ,  $y_{CO_2}$ ), did not improve predictive power over a reference Monod model (see Table 1). Additionally, refining the DOM pool into nine chemical classes with varying parameters did not lead to significant improvement in respiration predictions over the single pool model; the  $R^2$  values were similar between the two models (Table 1 and Figure 5). This might be because the model parameters were not significantly different between high and low DOM concentration soils (Figure S8), suggesting that respiration rates predicted across all soils were primarily driven by DOM concentration, rather than DOM chemistry.

Given that the MTS model does not explicitly account for DOM alpha diversity, we investigated whether the patterns observed in the regression model could emerge from MTS kinetics. Theoretically, MTS model predicts that an increase in DOM concentration,  $\mu_{max}$  or  $y_{OC}$  would increase respiration rate (Figure S9). From correlation analysis, we found a positive (but weak,  $r=0.34$ ,  $pval<0.01$ ) correlation between DOM and alpha diversity (Figure S10), and negative correlations between model parameters ( $\mu_{max}$  and  $y_{OC}$ ) with alpha diversity ( $r=[-0.47,-0.46]$  and  $pval<0.001$ , respectively, Figure S11). These findings suggest that soils with higher DOM concentrations and greater alpha diversity would exhibit lower values for these parameters, thus reducing respiration rates (Figure S9). In Supplementary Figure S12, we illustrate the respiration rate as a function of DOM using an arbitrary range of DOM concentrations and model parameters estimated from each soil sample. At very low DOM concentrations, the MTS model predicted an almost negligible respiration rate, indicating no effect of alpha diversity. Conversely, at high DOM concentrations, soils with relatively high alpha diversity were predicted to exhibit lower respiration rates. Therefore, the MTS model can potentially incorporate the effect of alpha diversity-respiration patterns found in regression model, however the parameterization based solely on DOM chemistry does not account for the effects of its chemodiversity. This is in line with Lehmann et al (2020), which posits that the decomposability of organic compounds is more contingent upon chemical diversity and organo-mineral interactions within soil than on the chemical properties of the organic compounds themselves.

Previous studies by Song et al. (2020) and Ahamed et al. (2023) employed a similar bioenergetic approach using MTS kinetics to leverage DOM chemodiversity in predicting microbial respiration rate from river systems. They utilized a fixed value of volume harvest parameter times substrate concentration (i.e.,  $V_h S_{DOC}$ ) in the denominator in the exponent of MTS kinetics (see Table 1). This approach did not account for the variability in DOM concentration across samples and resulted in a poor correlation between observed and simulated respiration rates compared to the results presented in this work. Building on these, Zheng et al. (2024), incorporated varying DOM concentration into an MTS kinetic model and tested different values of  $V_h$  to find the best correlation between simulated maximum growth rate (used as a proxy for respiration) and observed respiration rates. However, since the maximum growth rate (unit of  $\text{day}^{-1}$ ) and respiration rate (unit of  $\mu\text{mol CO}_2 \text{ g}^{-1} \text{ soil d}^{-1}$ ) are not directly comparable, a best fit parameter estimation of  $V_h$  was not performed in their studies, which may explain the low  $R^2 = 0.19$  between modeled maximum microbial growth rates and measured soil respiration rates.

#### **4.4. Implication and challenges for incorporating chemodiversity of DOM in biogeochemical models**

The factors driving the chemodiversity of DOM and its impact on microbial decomposition processes are intricately linked (Davenport et al., 2023; Lehmann and Kleber, 2015). Microbial niche separation, influenced by variations in substrates, mineralogy, moisture, temperature and other environmental factors, plays a critical role in shaping DOM chemodiversity (D'Andrilli et al., 2019; Kothawala et al., 2021; Logue et al., 2016; Wang et al., 2022). This complexity poses a substantial challenge for soil C models, particularly in determining the optimal level of detail required to represent DOM chemodiversity while preserving model simplicity. As a result, different modeling approaches to incorporate chemodiversity into process-based soil C cycle models have yielded divergent conclusions regarding its influence on DOM decomposition rates.

For instance, Weverka (2023) theorized that microorganisms might invest in a diverse enzyme set to assimilate heterogeneous DOM pools or selectively target more favorable substrates. Both strategies were shown to be associated with reduced overall C assimilation rates, thereby lowering DOM decomposition and microbial respiration. In contrast, Khurana et al. (2023) found a positive correlation between DOM chemodiversity and decomposition rate when chemodiversity was measured by the number of organic compounds, but not when assessed via variations in the nominal oxidation state of C in organic compounds. These examples highlight the necessity of improving DOM chemodiversity representation in models to capture its nonlinear effects on soil respiration. Another challenge involves microbial trait trade-offs due to varying DOM chemodiversity. Our results hints at the community level trade-offs between maximizing yield under resource-rich conditions versus prioritizing enzyme production under resource-depleted conditions. A potential solution for incorporating such trade-offs into models may involve dynamic optimization techniques that estimate optimal trait changes based on the chemical composition of organic matter (Chakrawal et al., 2024) or employing dynamic energy budget models to resolve the trade-off between microbial growth rate and CUE (Marschmann et al., 2024).

Adding detailed DOM chemistry to soil C cycling models also raises questions about whether this complexity truly enhances model performance, especially given the interactions with soil mineralogy and microbiology (Graham and Hofmockel, 2022). Recent studies, such as Muller et al. (2024), advocate for a more nuanced representation of DOM pools in mechanistic models. Muller et al. (2024) implemented a multi-pool DOM chemodiversity model in Lambda-PFLOTRAN, which can integrate biological and hydrological processes at the watershed scale, offering potential improvements for next-generation soil C cycling models, especially if expanded to represent variations in microbial functional traits tradeoff driven by DOM chemodiversity. While integrating detailed DOM chemistry in reactive transport or ecosystem-scale models is appealing, these frameworks often introduce additional parameters, which can lead to challenges like equifinality and parameter unidentifiability (Marschmann et al., 2019). Addressing these challenges requires widespread datasets with molecular scale resolution. Initiatives such as the Molecular Observation Network (MONet) are advancing high-throughput molecular-scale data collection, which could alleviate these data challenges. Future model development efforts that integrate these comprehensive datasets could substantially advance our understanding of molecular-scale processes and determine the requisite level of detail needed in large-scale Earth System Models.

## **5. Conclusions:**

Our findings reveal that, although there is a statistically significant relationship between DOM alpha diversity (a measure of chemodiversity) and soil respiration rates, kinetic models parameterized to reflect DOM chemodiversity failed to improve performance over the reference model using Monod kinetics. These contrasting results suggest that the impact of DOM chemistry on soil respiration is not adequately captured through substrate-specific model parameterization, even though emerging kinetic modeling approaches are theoretically capable of incorporating the feedbacks between DOM chemodiversity and microbial respiration. Accurately capturing the nonlinear effects of chemical diversity under varying resource conditions is essential for predicting soil C persistence as DOM chemodiversity may influence microbial metabolic trade-offs that affect C loss through respiration or retention as soil organic C.

## **6. Funding**

This research was performed at the Environmental Molecular Sciences Laboratory, a DOE Office of Science User Facility sponsored by the Biological and Environmental Research program under Contract No. DE-AC05-76RL01830.

## **7. Acknowledgments**

Soil data were provided by the Molecular Observation Network (MONet) at the Environmental Molecular Sciences Laboratory (<https://ror.org/04rc0xn13>), a DOE Office of Science user facility sponsored by the Biological and Environmental Research program under Contract No. DE-AC05-76RL01830. The work (proposal: 10.46936/10.25585/60008970) conducted by the U.S. Department of Energy, Joint Genome Institute (<https://ror.org/04xm1d337>), a DOE Office of Science user facility, is supported by the Office of Science of the U.S. Department of Energy operated under Contract No. DE-AC02-05CH11231. The Molecular Observation Network (MONet) database is an open, FAIR, and publicly available compilation of the molecular and microstructural properties of soil. Data in the MONet open science database can be

found at <https://sc-data.emsl.pnnl.gov/>. The National Ecological Observatory Network is a program sponsored by the National Science Foundation and operated under cooperative agreement by Battelle. A portion of soil samples collected for this research were obtained through NEON Research Support Services.

## 8. Data availability statement

All the data used in this analysis is available from the 1000 Soils Pilot Dataset repository <https://zenodo.org/records/7706774>, and scripts from <https://doi.org/10.5281/zenodo.15225636>.

## 9. References:

- Abramoff, R., Xu, X., Hartman, M., O'Brien, S., Feng, W., Davidson, E., Finzi, A., Moorhead, D., Schimel, J., Torn, M., Mayes, M.A., 2018. The Millennial model: in search of measurable pools and transformations for modeling soil carbon in the new century. *Biogeochemistry* 137, 51–71. <https://doi.org/10.1007/s10533-017-0409-7>
- Ahamed, F., You, Y., Burgin, A., Stegen, J.C., Scheibe, T.D., Song, H.-S., 2023. Exploring the determinants of organic matter bioavailability through substrate-explicit thermodynamic modeling. *Front. Water* 5. <https://doi.org/10.3389/frwa.2023.1169701>
- Amenabar, M.J., Shock, E.L., Roden, E.E., Peters, J.W., Boyd, E.S., 2017. Microbial substrate preference dictated by energy demand rather than supply. *Nat. Geosci.* 10, 577–581. <https://doi.org/10.1038/NGEO2978>
- Amend, J.P., LaRowe, D.E., 2019. Minireview: demystifying microbial reaction energetics. *Environ. Microbiol.* 21, 3539–3547. <https://doi.org/10.1111/1462-2920.14778>
- Anderson, C.G., Goebel, G.M., Tfaily, M.M., Fox, P.M., Nico, P.S., Fendorf, S., Keiluweit, M., 2023. Molecular Nature of Mineral-Organic Associations within Redox-Active Mountainous Floodplain Sediments. *ACS Earth Space Chem.* 7, 1623–1634. <https://doi.org/10.1021/acsearthspacechem.3c00037>
- Arel-Bundock, V., 2022. modelsummary: Data and Model Summaries in R. *J. Stat. Softw.* 103, 1–23. <https://doi.org/10.18637/jss.v103.i01>
- Ayala-Ortiz, C., Graf-Grachet, N., Freire-Zapata, V., Fudyma, J., Hildebrand, G., AminiTabrizi, R., Howard-Varona, C., Corilo, Y.E., Hess, N., Duhaime, M.B., Sullivan, M.B., Tfaily, M.M., 2023. MetaboDirect: an analytical pipeline for the processing of FT-ICR MS-based metabolomic data. *Microbiome* 11, 28. <https://doi.org/10.1186/s40168-023-01476-3>
- Bahureksa, W., Tfaily, M.M., Boiteau, R.M., Young, R.B., Logan, M.N., McKenna, A.M., Borch, T., 2021. Soil Organic Matter Characterization by Fourier Transform Ion Cyclotron Resonance Mass Spectrometry (FTICR MS): A Critical Review of Sample Preparation, Analysis, and Data Interpretation. *Environ. Sci. Technol.* 55, 9637–9656. <https://doi.org/10.1021/acs.est.1c01135>
- Bailey, V.L., Smith, A.P., Tfaily, M., Fansler, S.J., Bond-Lamberty, B., 2017. Differences in soluble organic carbon chemistry in pore waters sampled from different pore size domains. *Soil Biol. Biochem.* 107, 133–143. <https://doi.org/10.1016/j.soilbio.2016.11.025>
- Bowman, M.M., Heath, A.E., Varga, T., Battu, A.K., Chu, R.K., Toyoda, J., Cheeke, T.E., Porter, S.S., Moffett, K.B., LeTendre, B., Qafoku, O., Bargar, J.R., Mans, D.M., Hess, N.J., Graham, E.B., 2023. One thousand soils for molecular understanding of belowground carbon cycling. *Front. Soil Sci.* 3.
- Bowman, M.M., Heath, A.E., Varga, T., Battu, A.K., Kew, W., Shi, C., Chu, R., Toyoda, J., Qafoku, O., Bargar, J., Hess, N., Leichty, S., Townsend, A., Sconzo, N., Miller, P., Anderson, J., Stohel, I., Rosenstock,

- Mi., Lawver, A., Hauchambe, R., Clendinen, C., Wietsma, T., Graham, E.B., 2024. 1000 Soils Pilot Dataset, version 7, August 2024. <https://doi.org/10.5281/zenodo.13210467>
- Boye, K., Noël, V., Tfaily, M.M., Bone, S.E., Williams, K.H., Bargar, J.R., Fendorf, S., 2017. Thermodynamically controlled preservation of organic carbon in floodplains. *Nat. Geosci.* 10, 415–419. <https://doi.org/10.1038/ngeo2940>
- Camino-Serrano, M., Guenet, B., Luysaert, S., Ciais, P., Bastrikov, V., Vos, B.D., Gielen, B., Gleixner, G., Jornet-Puig, A., Kaiser, K., Kothawala, D., Lauerwald, R., Peñuelas, J., Schrumpf, M., Vicca, S., Vuichard, N., Walmsley, D., Janssens, I.A., 2018. ORCHIDEE-SOM: modeling soil organic carbon (SOC) and dissolved organic carbon (DOC) dynamics along vertical soil profiles in Europe. *Geosci. Model Dev.* 11, 937–957. <https://doi.org/10.5194/gmd-11-937-2018>
- Chakrawal, A., Calabrese, S., Herrmann, A.M., Manzoni, S., 2022. Interacting Bioenergetic and Stoichiometric Controls on Microbial Growth. *Front. Microbiol.* 13.
- Chakrawal, A., Herrmann, A.M., Šantrůčková, H., Manzoni, S., 2020. Quantifying microbial metabolism in soils using calorimetry — A bioenergetics perspective. *Soil Biol. Biochem.* 107945. <https://doi.org/10.1016/j.soilbio.2020.107945>
- Chakrawal, A., Lindahl, B.D., Manzoni, S., 2024. Modelling optimal ligninolytic activity during plant litter decomposition. *New Phytol.* n/a. <https://doi.org/10.1111/nph.19572>
- Cui, Y., Wen, S., Stegen, J.C., Hu, A., Wang, J., 2024. Chemodiversity of riverine dissolved organic matter: Effects of local environments and watershed characteristics. *Water Res.* 250, 121054. <https://doi.org/10.1016/j.watres.2023.121054>
- Danczak, R.E., Garayburu-Caruso, V.A., Renteria, L., McKeever, S.A., Otenburg, O.C., Grieger, S.R., Son, K., Kaufman, M.H., Fulton, S.G., Roebuck, J.A., Myers-Pigg, A.N., Stegen, J.C., 2023. Riverine organic matter functional diversity increases with catchment size. *Front. Water* 5. <https://doi.org/10.3389/frwa.2023.1087108>
- D'Andrilli, J., Junker, J.R., Smith, H.J., Scholl, E.A., Foreman, C.M., 2019. DOM composition alters ecosystem function during microbial processing of isolated sources. *Biogeochemistry* 142, 281–298. <https://doi.org/10.1007/s10533-018-00534-5>
- Dao, T.T., Mikutta, R., Sauheitl, L., Gentsch, N., Shibistova, O., Wild, B., Schneckner, J., Bárta, J., Čapek, P., Gittel, A., Lashchinskiy, N., Ulrich, T., Šantrůčková, H., Richter, A., Guggenberger, G., 2022. Lignin Preservation and Microbial Carbohydrate Metabolism in Permafrost Soils. *J. Geophys. Res. Biogeosciences* 127, e2020JG006181. <https://doi.org/10.1029/2020JG006181>
- Davenport, R., Bowen, B.P., Lynch, L.M., Kosina, S.M., Shabtai, I., Northen, T.R., Lehmann, J., 2023. Decomposition decreases molecular diversity and ecosystem similarity of soil organic matter. *Proc. Natl. Acad. Sci.* 120, e2303335120. <https://doi.org/10.1073/pnas.2303335120>
- del Cerro, C., Erickson, E., Dong, T., Wong, A.R., Eder, E.K., Purvine, S.O., Mitchell, H.D., Weitz, K.K., Markillie, L.M., Burnet, M.C., Hoyt, D.W., Chu, R.K., Cheng, J.-F., Ramirez, K.J., Katahira, R., Xiong, W., Himmel, M.E., Subramanian, V., Linger, J.G., Salvachúa, D., 2021. Intracellular pathways for lignin catabolism in white-rot fungi. *Proc. Natl. Acad. Sci.* 118, e2017381118. <https://doi.org/10.1073/pnas.2017381118>
- Desmond-Le Quémener, E., Bouchez, T., 2014. A thermodynamic theory of microbial growth. *ISME J.* 8, 1747–1751. <https://doi.org/10.1038/ismej.2014.7>
- Ding, Y., Shi, Z., Ye, Q., Liang, Y., Liu, M., Dang, Z., Wang, Y., Liu, C., 2020. Chemodiversity of Soil Dissolved Organic Matter. *Environ. Sci. Technol.* 54, 6174–6184. <https://doi.org/10.1021/acs.est.0c01136>
- Freeman, E.C., Emilson, E.J.S., Dittmar, T., Braga, L.P.P., Emilson, C.E., Goldhammer, T., Martineau, C., Singer, G., Tanentzap, A.J., 2024. Universal microbial reworking of dissolved organic matter along environmental gradients. *Nat. Commun.* 15, 187. <https://doi.org/10.1038/s41467-023-44431-4>

- González-Cabaleiro, R., Ofițeru, I.D., Lema, J.M., Rodríguez, J., 2015. Microbial catabolic activities are naturally selected by metabolic energy harvest rate. *ISME J.* 9, 2630–2641. <https://doi.org/10.1038/ismej.2015.69>
- Graham, E.B., Hofmockel, K.S., 2022. Ecological stoichiometry as a foundation for omics-enabled biogeochemical models of soil organic matter decomposition. *Biogeochemistry* 157, 31–50. <https://doi.org/10.1007/s10533-021-00851-2>
- Gunina, A., Kuzyakov, Y., 2021. From energy to (soil organic) matter. *Glob. Change Biol.* n/a. <https://doi.org/10.1111/gcb.16071>
- Hall, S.J., Huang, W., Timokhin, V.I., Kenneth E. Hammel, 2020a. Lignin lags, leads, or limits the decomposition of litter and soil organic carbon. *Ecology* 101, e03113. <https://doi.org/10.1002/ecy.3113>
- Hall, S.J., Ye, C., Weintraub, S.R., Hockaday, W.C., 2020b. Molecular trade-offs in soil organic carbon composition at continental scale. *Nat. Geosci.* 13, 687–692. <https://doi.org/10.1038/s41561-020-0634-x>
- Kalbitz, K., Schwesig, D., Schmerwitz, J., Kaiser, K., Haumaier, L., Glaser, B., Ellerbrock, R., Leinweber, P., 2003. Changes in properties of soil-derived dissolved organic matter induced by biodegradation. *Soil Biol. Biochem.* 35, 1129–1142. [https://doi.org/10.1016/S0038-0717\(03\)00165-2](https://doi.org/10.1016/S0038-0717(03)00165-2)
- Keiluweit, M., Bougoure, J.J., Nico, P.S., Pett-Ridge, J., Weber, P.K., Kleber, M., 2015. Mineral protection of soil carbon counteracted by root exudates. *Nat. Clim. Change* 5, 588–595. <https://doi.org/10.1038/nclimate2580>
- Khurana, S., Abramoff, R., Bruni, E., Dondini, M., Tupek, B., Guenet, B., Lehtonen, A., Manzoni, S., 2023. Interactive effects of microbial functional diversity and carbon availability on decomposition – A theoretical exploration. *Ecol. Model.* 486, 110507. <https://doi.org/10.1016/j.ecolmodel.2023.110507>
- Kirk, T.K., Farrell, R.L., 1987. Enzymatic “Combustion”: The Microbial Degradation of Lignin. *Annu. Rev. Microbiol.* 41, 465–501. <https://doi.org/10.1146/annurev.mi.41.100187.002341>
- Kleerebezem, R., Van Loosdrecht, M.C., 2010. A generalized method for thermodynamic state analysis of environmental systems. *Crit. Rev. Environ. Sci. Technol.* 40, 1–54. <https://doi.org/10.1080/10643380802000974>
- Kothawala, D.N., Kellerman, A.M., Catalán, N., Tranvik, L.J., 2021. Organic Matter Degradation across Ecosystem Boundaries: The Need for a Unified Conceptualization. *Trends Ecol. Evol.* 36, 113–122. <https://doi.org/10.1016/j.tree.2020.10.006>
- LaRowe, D.E., Van Cappellen, P., 2011. Degradation of natural organic matter: A thermodynamic analysis. *Geochim. Cosmochim. Acta* 75, 2030–2042. <https://doi.org/10.1016/j.gca.2011.01.020>
- Lehmann, J., Hansel, C.M., Kaiser, C., Kleber, M., Maher, K., Manzoni, S., Nunan, N., Reichstein, M., Schimel, J.P., Torn, M.S., Wieder, W.R., Kögel-Knabner, I., 2020. Persistence of soil organic carbon caused by functional complexity. *Nat. Geosci.* 13, 529–534. <https://doi.org/10.1038/s41561-020-0612-3>
- Lehmann, J., Kleber, M., 2015. The contentious nature of soil organic matter. *Nature*. <https://doi.org/10.1038/nature16069>
- Li, P., Wu, M., Li, T., Dumbrell, A.J., Saleem, M., Kuang, L., Luan, L., Wang, S., Li, Z., Jiang, J., 2023. Molecular weight of dissolved organic matter determines its interactions with microbes and its assembly processes in soils. *Soil Biol. Biochem.* 184, 109117. <https://doi.org/10.1016/j.soilbio.2023.109117>
- Logue, J.B., Stedmon, C.A., Kellerman, A.M., Nielsen, N.J., Andersson, A.F., Laudon, H., Lindström, E.S., Kritzberg, E.S., 2016. Experimental insights into the importance of aquatic bacterial community

- composition to the degradation of dissolved organic matter. *ISME J.* 10, 533–545.  
<https://doi.org/10.1038/ismej.2015.131>
- Lv, J., Huang, Z., Christie, P., Zhang, S., 2020. Reducing Reagents Induce Molecular Artifacts in the Extraction of Soil Organic Matter. *ACS Earth Space Chem.* 4, 1913–1919.  
<https://doi.org/10.1021/acsearthspacechem.0c00194>
- Malik, A.A., Martiny, J.B.H., Brodie, E.L., Martiny, A.C., Treseder, K.K., Allison, S.D., 2020. Defining trait-based microbial strategies with consequences for soil carbon cycling under climate change. *ISME J.* 14, 1–9. <https://doi.org/10.1038/s41396-019-0510-0>
- Manzoni, S., Cotrufo, M.F., 2024. Mechanisms of soil organic carbon and nitrogen stabilization in mineral-associated organic matter – insights from modeling in phase space. *Biogeosciences* 21, 4077–4098. <https://doi.org/10.5194/bg-21-4077-2024>
- Marschmann, G.L., Pagel, H., Kügler, P., Streck, T., 2019. Equifinality, sloppiness, and emergent structures of mechanistic soil biogeochemical models. *Environ. Model. Softw.* 122, 104518.  
<https://doi.org/10.1016/j.envsoft.2019.104518>
- Marschmann, G.L., Tang, J., Zhalnina, K., Karaoz, U., Cho, H., Le, B., Pett-Ridge, J., Brodie, E.L., 2024. Predictions of rhizosphere microbiome dynamics with a genome-informed and trait-based energy budget model. *Nat. Microbiol.* 9, 421–433. <https://doi.org/10.1038/s41564-023-01582-w>
- Mattila, H., Österman-Udd, J., Mali, T., Lundell, T., 2022. Basidiomycota Fungi and ROS: Genomic Perspective on Key Enzymes Involved in Generation and Mitigation of Reactive Oxygen Species. *Front. Fungal Biol.* 3.
- Mayes, M.A., Heal, K.R., Brandt, C.C., Phillips, J.R., Jardine, P.M., 2012. Relation between Soil Order and Sorption of Dissolved Organic Carbon in Temperate Subsoils. *Soil Sci. Soc. Am. J.* 76, 1027–1037.  
<https://doi.org/10.2136/sssaj2011.0340>
- McGowen, E.B., Sharma, S., Deng, S., Zhang, H., Warren, J.G., 2018. An Automated Laboratory Method for Measuring CO<sub>2</sub> Emissions from Soils. *Agric. Environ. Lett.* 3, 180008.  
<https://doi.org/10.2134/aer2018.02.0008>
- Muller, K.A., Jiang, P., Hammond, G., Ahmadullah, T., Song, H.-S., Kukkadapu, R., Ward, N., Bowe, M., Chu, R.K., Zhao, Q., Garayburu-Caruso, V.A., Roebuck, A., Chen, X., 2024. Lambda-PFLOTRAN 1.0: Workflow for Incorporating Organic Matter Chemistry Informed by Ultra High Resolution Mass Spectrometry into Biogeochemical Modeling. <https://doi.org/10.5194/gmd-2024-34>
- Negassa, W., Eckhardt, K.-U., Regier, T., Leinweber, P., 2021. Dissolved organic matter concentration, molecular composition, and functional groups in contrasting management practices of peatlands. *J. Environ. Qual.* 50, 1364–1380. <https://doi.org/10.1002/jeq2.20284>
- Nunan, N., Schmidt, H., Raynaud, X., 2020. The ecology of heterogeneity: soil bacterial communities and C dynamics. *Philos. Trans. R. Soc. B Biol. Sci.* 375, 20190249.  
<https://doi.org/10.1098/rstb.2019.0249>
- Parton, W.J., Ojima, D.S., Cole, C.V., Schimel, D.S., 1994. A General Model for Soil Organic Matter Dynamics: Sensitivity to Litter Chemistry, Texture and Management, in: *Quantitative Modeling of Soil Forming Processes*. John Wiley & Sons, Ltd, pp. 147–167.
- Robertson, A.D., Paustian, K., Ogle, S., Wallenstein, M.D., Lugato, E., Cotrufo, M.F., 2019. Unifying soil organic matter formation and persistence frameworks: the MEMS model. *Biogeosciences* 16, 1225–1248. <https://doi.org/10.5194/bg-16-1225-2019>
- Schmidt, M.W.I., Torn, M.S., Abiven, S., Dittmar, T., Guggenberger, G., Janssens, I.A., Kleber, M., Kögel-Knabner, I., Lehmann, J., Manning, D.A.C., Nannipieri, P., Rasse, D.P., Weiner, S., Trumbore, S.E., 2011. Persistence of soil organic matter as an ecosystem property. *Nature* 478, 49–56.  
<https://doi.org/10.1038/nature10386>

- Scott, M., Gunderson, C.W., Mateescu, E.M., Zhang, Z., Hwa, T., 2010. Interdependence of Cell Growth and Gene Expression: Origins and Consequences. *Science* 330, 1099–1102. <https://doi.org/10.1126/science.1192588>
- Shi, C., Mudunuru, M., Bowman, M., Zhao, Q., Toyoda, J., Kew, W., Corilo, Y., Qafoku, O., Bargar, J.R., Karra, S., Graham, E.B., 2025. Scaling High-Resolution Soil Organic Matter Composition to Improve Predictions of Potential Soil Respiration Across the Continental United States. *Geophys. Res. Lett.* 52, e2024GL113091. <https://doi.org/10.1029/2024GL113091>
- Sinsabaugh, R.L., Hill, B.H., Follstad Shah, J.J., 2009. Ecoenzymatic stoichiometry of microbial organic nutrient acquisition in soil and sediment. *Nature* 462, 795–798. <https://doi.org/10.1038/nature08632>
- Sokol, N.W., Sanderman, J., Bradford, M.A., 2019. Pathways of mineral-associated soil organic matter formation: Integrating the role of plant carbon source, chemistry, and point of entry. *Glob. Change Biol.* 25, 12–24. <https://doi.org/10.1111/gcb.14482>
- Song, H.-S., Stegen, J.C., Graham, E.B., Lee, J.-Y., Garayburu-Caruso, V.A., Nelson, W.C., Chen, X., Moulton, J.D., Scheibe, T.D., 2020. Representing Organic Matter Thermodynamics in Biogeochemical Reactions via Substrate-Explicit Modeling. *Front. Microbiol.* 11. <https://doi.org/10.3389/fmicb.2020.531756>
- Tanentzap, A.J., Fonvielle, J.A., 2024. Chemodiversity in freshwater health. *Science* 383, 1412–1414. <https://doi.org/10.1126/science.adg8658>
- Thevenot, M., Dignac, M.-F., Rumpel, C., 2010. Fate of lignins in soils: A review. *Soil Biol. Biochem.* 42, 1200–1211. <https://doi.org/10.1016/j.soilbio.2010.03.017>
- Ugalde-Salas, P., Desmond-Le Quéméner, E., Harmand, J., Rapaport, A., Bouchez, T., 2020. Insights from Microbial Transition State Theory on Monod’s Affinity Constant. *Sci. Rep.* 10, 5323. <https://doi.org/10.1038/s41598-020-62213-6>
- Wang, G., Post, W.M., Mayes, M.A., 2013. Development of microbial-enzyme-mediated decomposition model parameters through steady-state and dynamic analyses. *Ecol. Appl.* 23, 255–272. <https://doi.org/10.1890/12-0681.1>
- Wang, Y., Xie, R., Shen, Y., Cai, R., He, C., Chen, Q., Guo, W., Shi, Q., Jiao, N., Zheng, Q., 2022. Linking Microbial Population Succession and DOM Molecular Changes in Synechococcus-Derived Organic Matter Addition Incubation. *Microbiol. Spectr.* 10, e02308-21. <https://doi.org/10.1128/spectrum.02308-21>
- Weverka, J.R., Moeller, H.V., Schimel, J.P., 2023. Chemodiversity controls microbial assimilation of soil organic carbon: A theoretical model. *Soil Biol. Biochem.* 187, 109161. <https://doi.org/10.1016/j.soilbio.2023.109161>
- Wieder, W.R., Grandy, A.S., Kallenbach, C.M., Bonan, G.B., 2014. Integrating microbial physiology and physio-chemical principles in soils with the Microbial-MIneral Carbon Stabilization (MIMICS) model. *Biogeosciences* 11, 3899–3917. <https://doi.org/10.5194/bg-11-3899-2014>
- Witzgall, K., Vidal, A., Schubert, D.I., Höschen, C., Schweizer, S.A., Buegger, F., Pouteau, V., Chenu, C., Mueller, C.W., 2021. Particulate organic matter as a functional soil component for persistent soil organic carbon. *Nat. Commun.* 12, 4115. <https://doi.org/10.1038/s41467-021-24192-8>
- Yang, X., Zhang, S., Wu, D., Huang, Y., Zhang, L., Liu, K., Wu, H., Guo, S., Zhang, W., 2024. Recalcitrant components accumulation in dissolved organic matter decreases microbial metabolic quotient of red soil under long-term manuring. *Sci. Total Environ.* 934, 173287. <https://doi.org/10.1016/j.scitotenv.2024.173287>
- Yu, L., Ahrens, B., Wutzler, T., Schrumpf, M., Zaehle, S., 2020. Jena Soil Model (JSM v1.0; revision 1934): a microbial soil organic carbon model integrated with nitrogen and phosphorus processes. *Geosci. Model Dev.* 13, 783–803. <https://doi.org/10.5194/gmd-13-783-2020>

Zheng, J., Scheibe, T.D., Boye, K., Song, H.-S., 2024. Thermodynamic control on the decomposition of organic matter across different electron acceptors. *Soil Biol. Biochem.* 193, 109364. <https://doi.org/10.1016/j.soilbio.2024.109364>

Zhou, L., Zhou, Y., Tang, X., Zhang, Y., Jang, K.-S., Székely, A.J., Jeppesen, E., 2021. Resource aromaticity affects bacterial community successions in response to different sources of dissolved organic matter. *Water Res.* 190, 116776. <https://doi.org/10.1016/j.watres.2020.116776>

## Supplementary information

Challenges in Integrating Dissolved Organic Matter Chemodiversity into Kinetic Models of Soil Respiration

Arjun Chakrawal<sup>1</sup>, Odeta Qafoku<sup>1</sup>, Satish Karra<sup>1</sup>, John Bargar<sup>1</sup>, and Emily Graham<sup>1,2</sup>

<sup>1</sup>Environmental Molecular Sciences Laboratory (EMSL), Pacific Northwest National Laboratory, PO Box 999, Richland, WA 99352, USA

<sup>2</sup>School of Biological Sciences, Washington State University, Pullman, WA, USA

### 10. Nominal oxidation state of carbon, double bond equivalent, modified aromatic index

The nominal oxidation state of carbon (NOSC) in an organic compound ( $C_aH_bN_cO_dP_eS_f^z$ ) is defined as following,

$$NOSC = 4 - \frac{4a + b - 3c - 2d + 5e - 2f - n_z}{a} \quad (A10)$$

The NOSC ranges from -4 for most reduced state of C in  $CH_4$  and +4 for most oxidized state of C in  $CO_2$  (LaRowe and Van Cappellen, 2011).

The double bond equivalent (*DBE*) is used to estimate the degree of unsaturation (i.e., the presence of double, triple bond or rings in chemical structure) in an organic compound (Koch and Dittmar, 2006) and calculated as follows,

$$DBE = 1 + 0.5(2a - b + c) \quad (A11)$$

The modified aromaticity index is estimated as follows,

$$AI_{mod} = \frac{1 + a - d - f - 0.5(b + c)}{a - d - f - c} \quad (A12)$$

### 11. Shannon diversity index

Shannon diversity index (*Sh*) provides a measure of entropy of the population, here, the population is chemically diverse DOM, and calculated as,

$$Sh = \sum_{i=1}^n p_i \ln p_i \quad (A13)$$

where  $n=9$  is the total number of chemical classes, and  $p_i$  is the relative abundance of each chemical class.

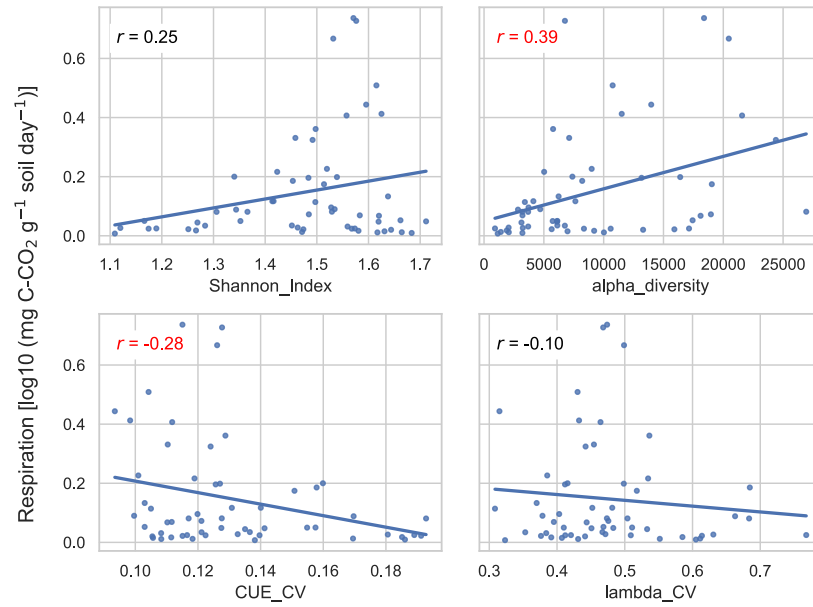


Figure S1 Scatter plots with regression lines showing relationships between soil respiration and proxies of chemodiversity Shannon and alpha diversity, coefficient of variations of CUE and thermodynamic factor (lambda\_CV). Pearson correlation coefficients ('r') are annotated; red indicates significance, black indicates non-significance.

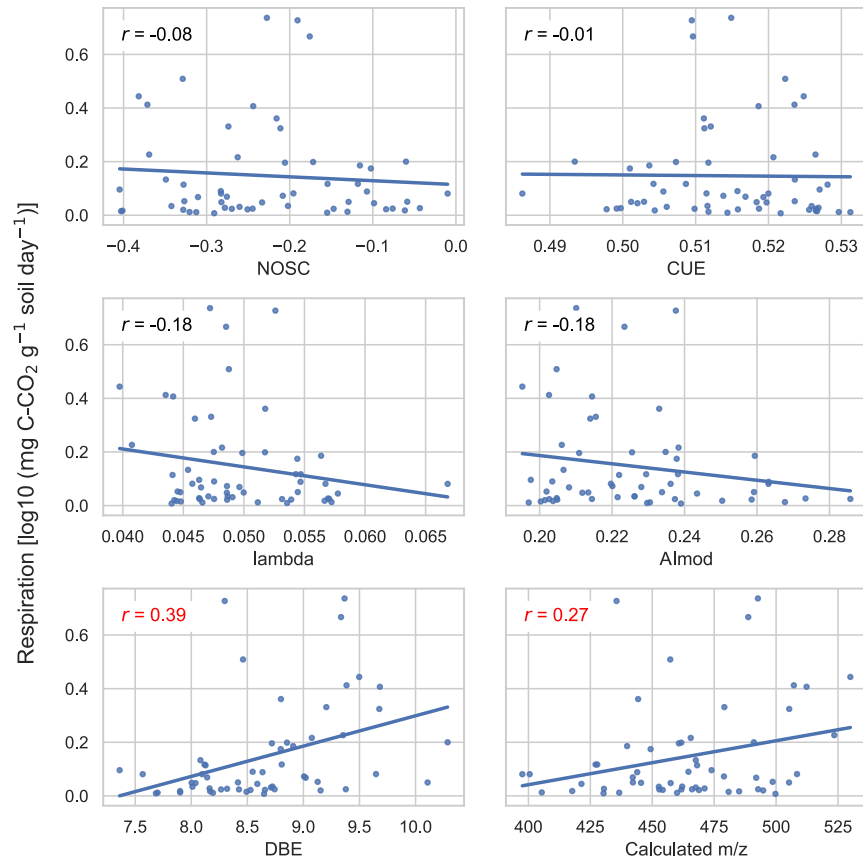


Figure S2 Relationship between variables describing chemical nature of DOM and respiration. NOSC (nominal oxidation state of carbon), CUE (C use efficiency), lambda (thermodynamic factor), Almod (aromaticity index), DBE (double bond equivalents), and calculated m/z (mass-to-charge ratio). Pearson correlation coefficients ('r') are annotated; red indicates significance, black indicates non-significance.

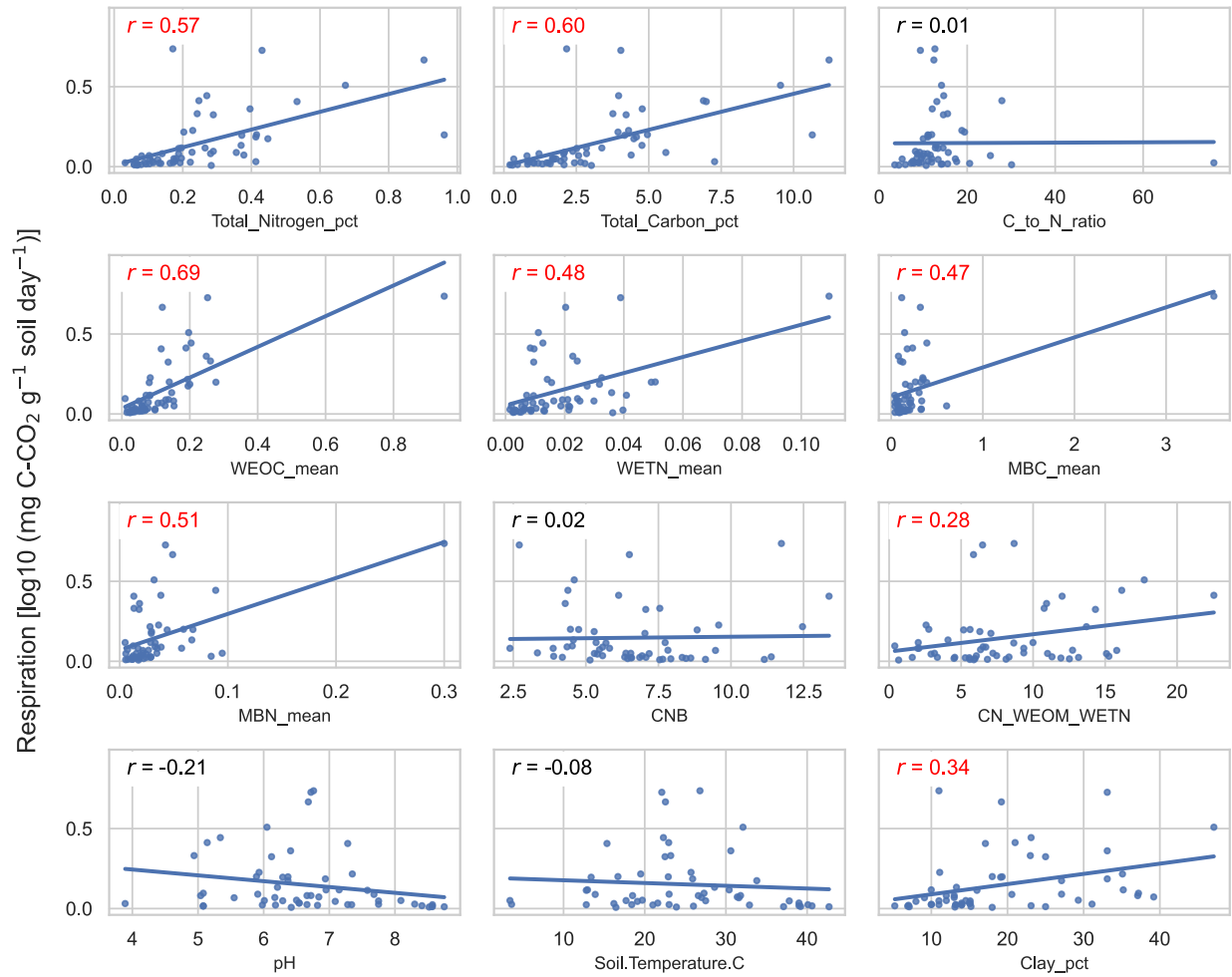


Figure S3 Relationship between respiration rate and biogeochemical predictors. Pearson correlation coefficients ( $r$ ) are annotated; red indicates significance, black indicates non-significance.

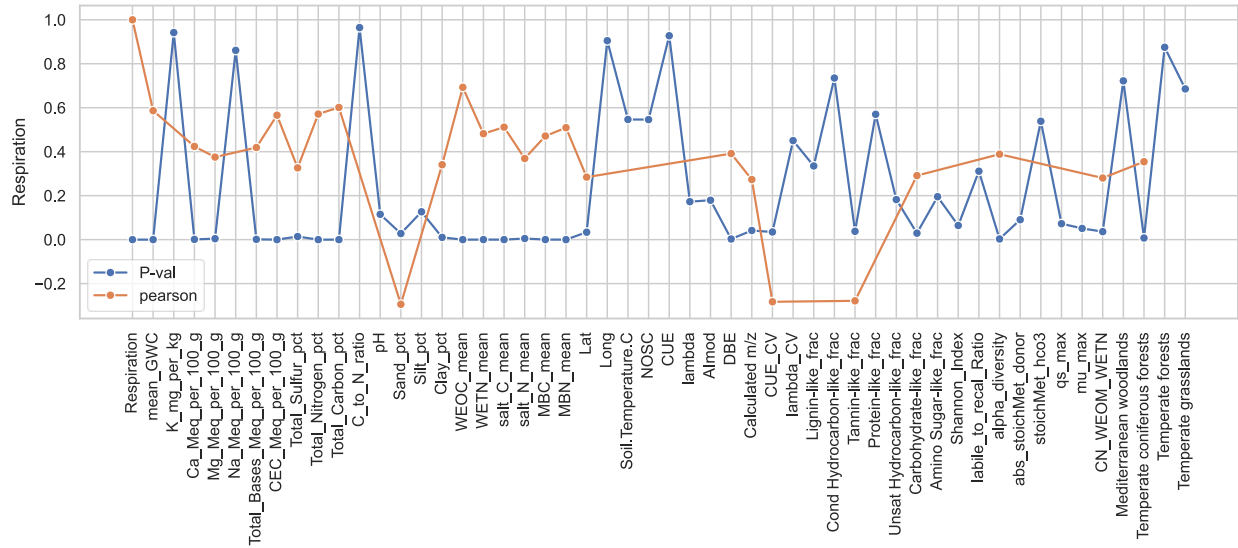


Figure S4 Pearson correlation coefficient and p-value between respiration rate and other predictors.

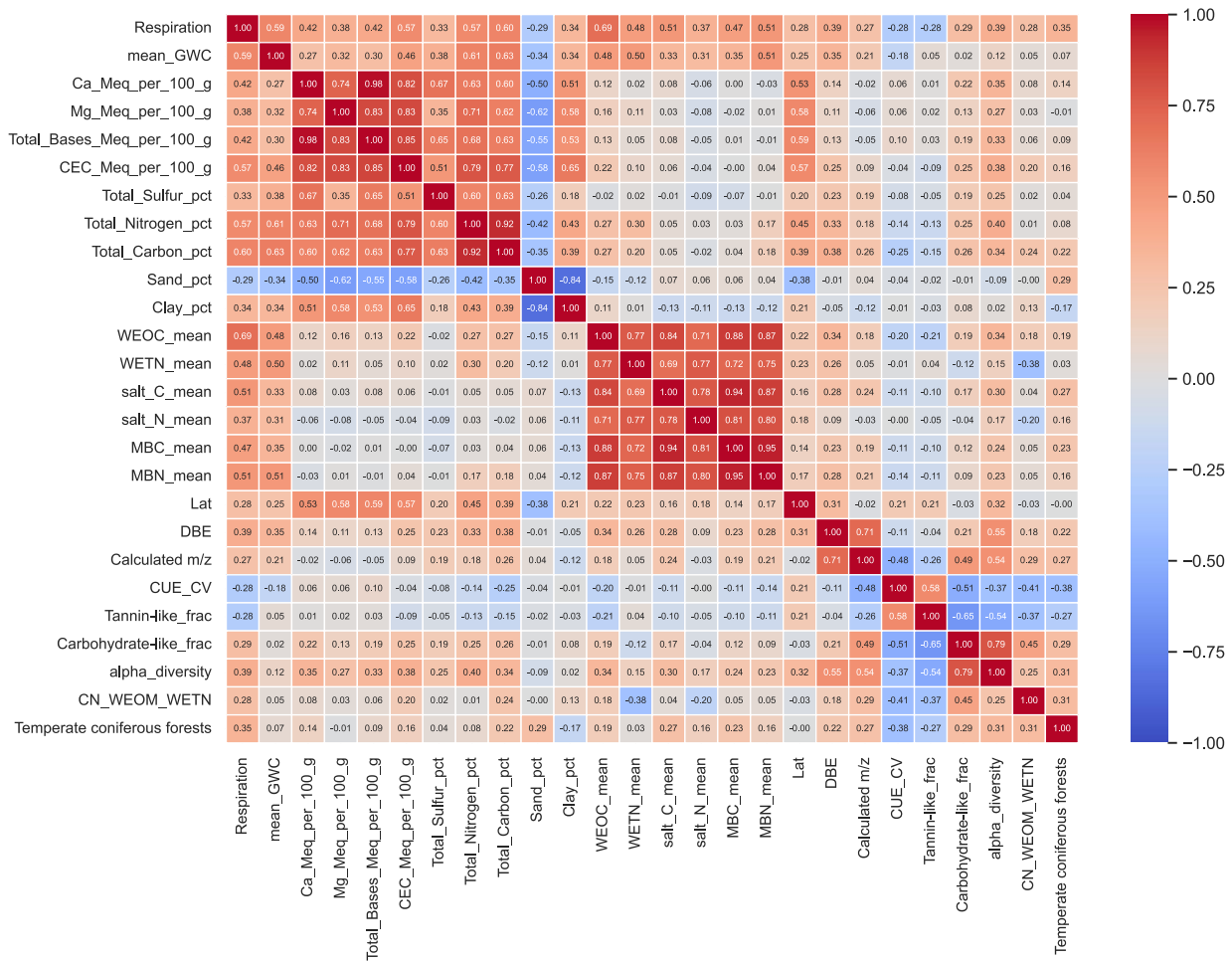


Figure S5 Heatmap of Pearson correlation matrix among predictor and respiration rate after removing insignificant predictor (p-val>0.05) from Figure S4.

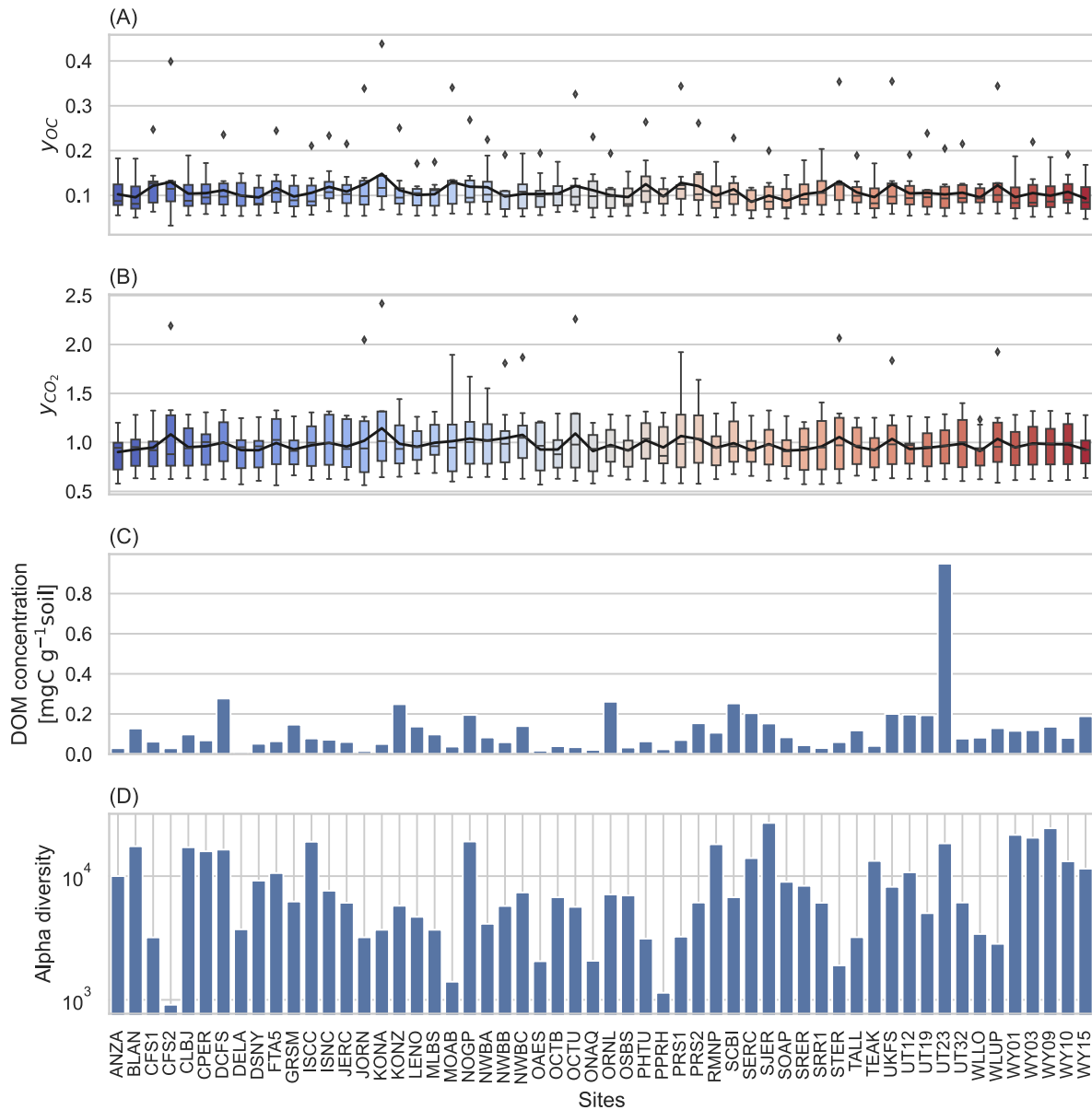


Figure S6 Stoichiometry of organic compound  $y_{OC}$  (A) and  $CO_2$   $y_{CO_2}$  (B) in the metabolic growth reaction, DOM concentration (C), and alpha diversity, i.e., species richness of DOM for each soil sample (D). The box plots of  $y_{OC}$  and  $y_{CO_2}$  show the variation across different chemical classes, and the solid black line is the mean value.

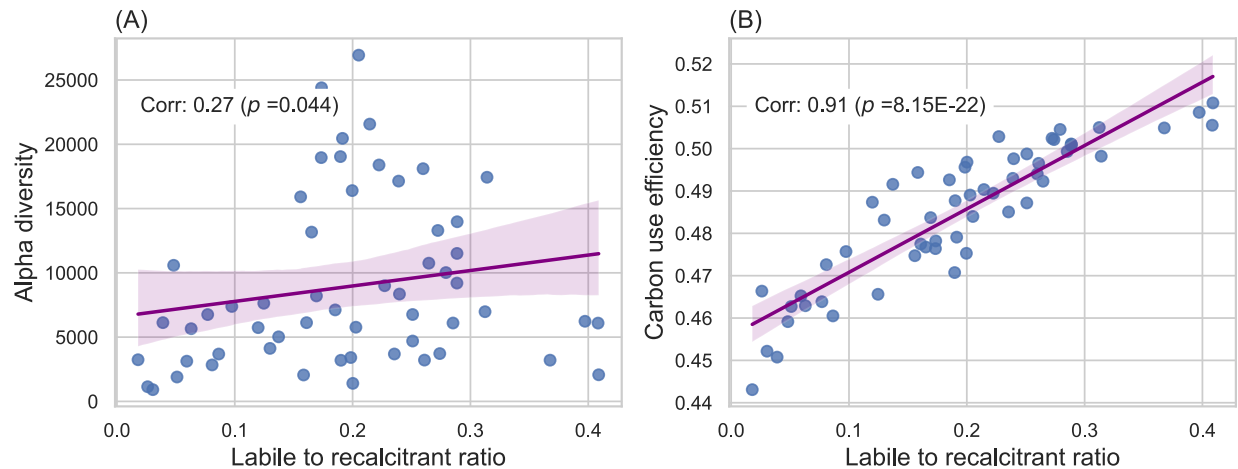


Figure S7 Alpha diversity of DOM (A) and carbon use efficiency (B) as a function of the ratio of labile to recalcitrant organic compounds. Carbohydrates-like, proteins-like, amino sugars-like, lipids-like, unsaturated hydrocarbons-like, and other compounds were taken as labile pools, whereas lignin-like, condensed hydrocarbons-like, and tannins-like were considered as recalcitrant compounds. The annotated text, *Corr* and *p*, denote the Spearman correlation and corresponding p-value, respectively.

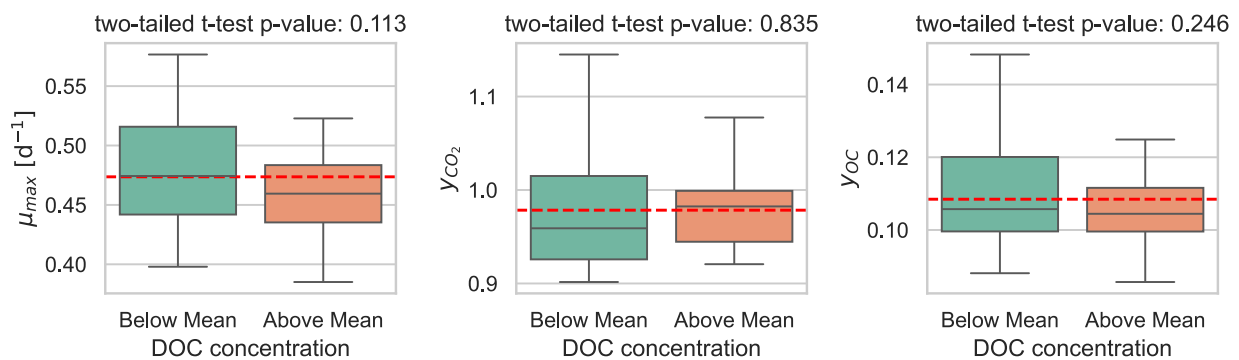


Figure S8 Boxplots of maximum growth rate ( $\mu_{max}$ ), stoichiometric coefficient of CO<sub>2</sub> and OC for soils classified as DOM concentration below or above the average value. A two-sided t-test was conducted to assess whether the mean values of each variable differ significantly between the two soil categories. The red line represents the average value of each variable across all soil samples.

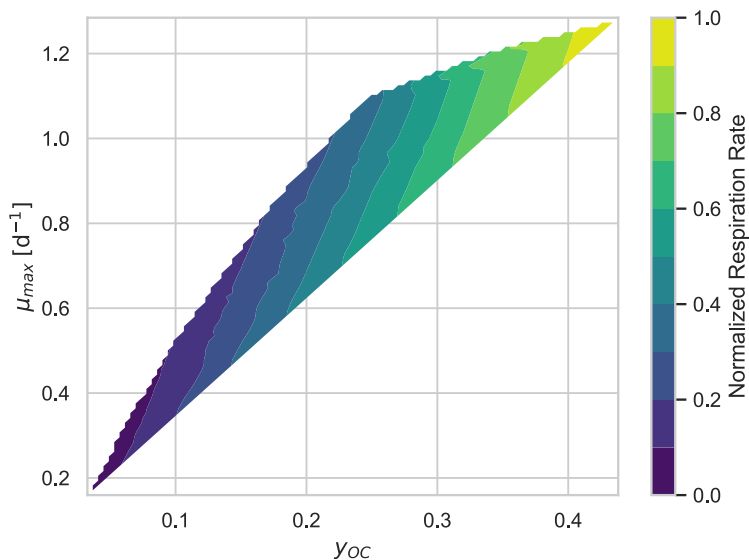


Figure S9 Variation in simulated respiration rate  $(R_{\text{norm}} = R/N = \mu_{\text{max}}(y_{\text{OC}}a - 1) \exp(-\frac{y_{\text{OC}}}{V_h S_{\text{DOC}}}))$  for varying values of observed  $y_{\text{OC}}$  and  $\mu_{\text{max}}$  obtained from FTICR-MS data. We fixed  $N$  and  $V_h$  value to 1.

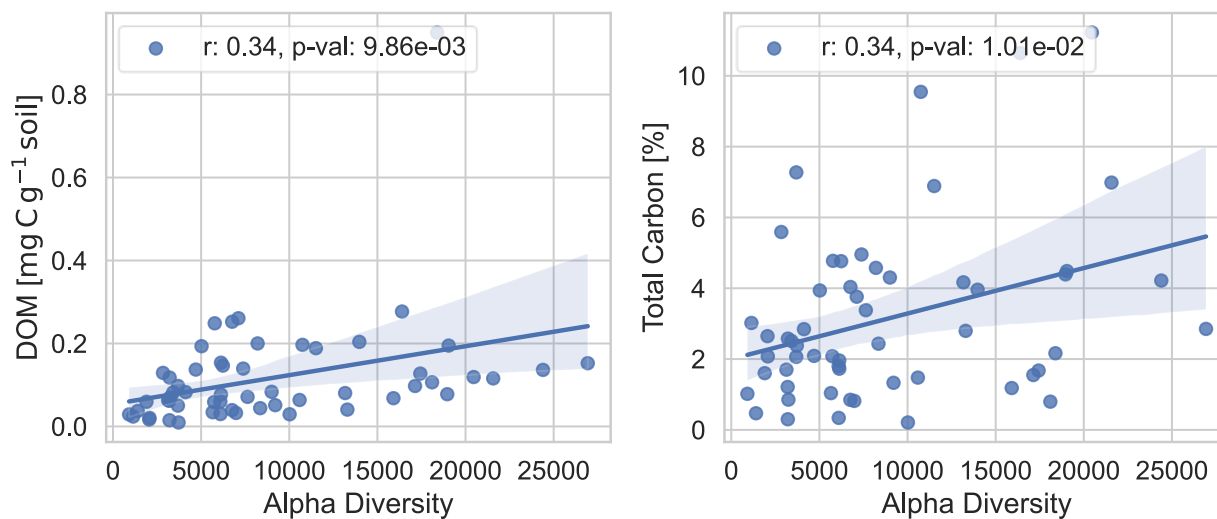


Figure S10 Scatterplot with a regression line showing relationship between DOM concentration and total C % with alpha diversity.

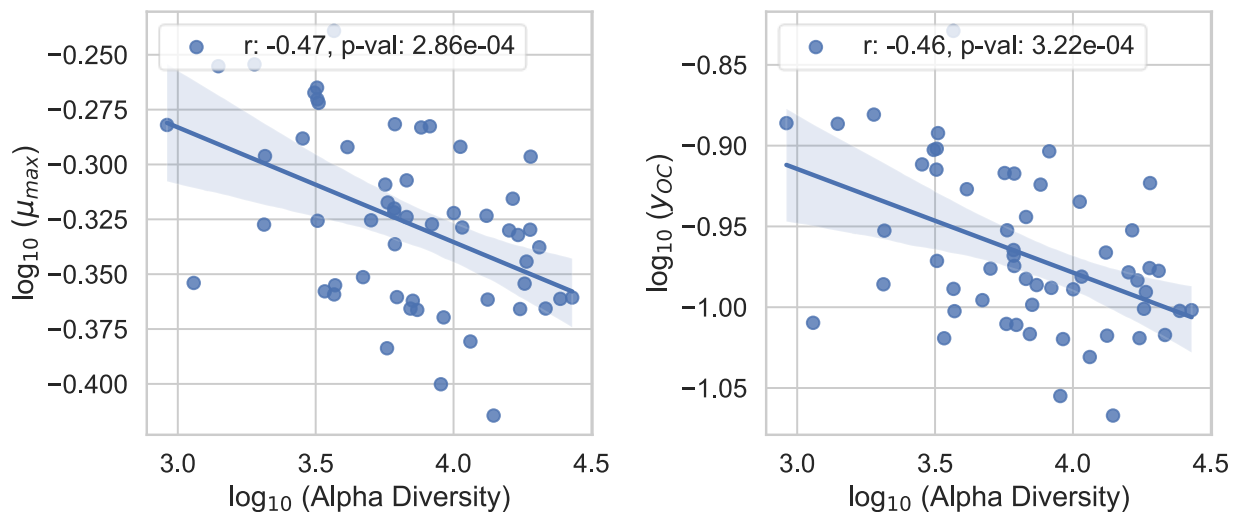


Figure S11 Scatterplot with a regression line showing relationship between  $\mu_{max}$  and  $y_{OC}$  with alpha diversity.

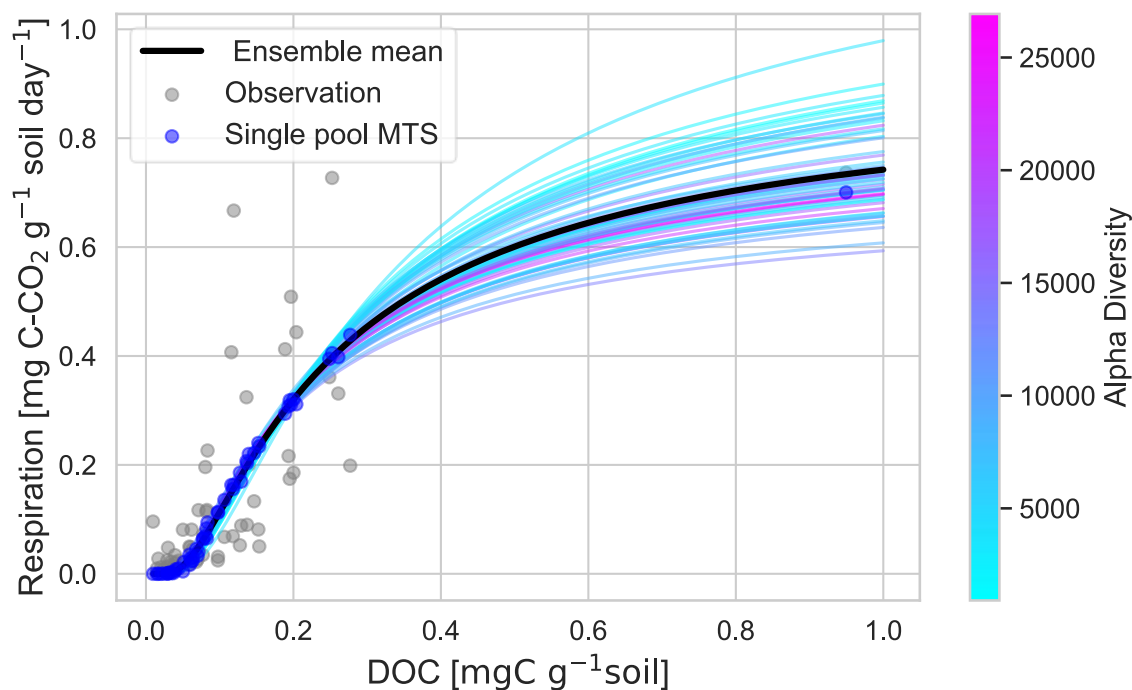


Figure S12 Modeled and observed soil respiration as a function of dissolved organic matter (DOM) concentration. The colored lines represent 56 realizations of respiration rate generated using a single-pool Metabolic transition theory kinetic (MTS, eq 8), with colors indicating alpha diversity. In each realization, respiration was simulated by varying the stoichiometric coefficient of organic carbon ( $y_{OC}$ ), the stoichiometric coefficient of CO<sub>2</sub> ( $y_{CO_2}$ ), and the maximum growth rate ( $\mu_{max}$ ) across observed soil

values, while holding the best-fit parameters  $N$  and  $V_h$  constant from the MTS Single pool main text Table 1. The black line represents the ensemble mean across realizations. Observed respiration rates are shown as grey scatter points, while the predicted respiration from the fitted single-pool MTS model is shown in blue. The color bar denotes alpha diversity, highlighting its variation across realizations. Each line represents the respiration kinetics for a given soil. Note that most soil with alpha diversity model parameters are such that respiration rate is lower (reddish blue lines below black line).

Table S1 Coefficient estimates and model fit statistics from linear regression for predicting respiration across different models during model selection process

|                                       | (1)                | (2)                | (3)                | (4)                | (5)                | (6) Final          |
|---------------------------------------|--------------------|--------------------|--------------------|--------------------|--------------------|--------------------|
| (Intercept)                           | -1.01<br>(0.06)*** | -1.02<br>(0.06)*** | -1.07<br>(0.04)*** | -1.08<br>(0.05)*** | -1.04<br>(0.05)*** | -1.06<br>(0.04)*** |
| Total_Carbon_pct                      | 0.21 (0.12)+       | 0.15 (0.09)        | 0.16 (0.06)*       | 0.19 (0.06)**      | 0.17 (0.06)**      | 0.16 (0.05)**      |
| DOM_conc                              | 0.29 (0.15)+       | 0.47<br>(0.11)***  | 0.56<br>(0.08)***  | 0.52<br>(0.08)***  | 0.52<br>(0.08)***  | 0.55<br>(0.07)***  |
| CN_ratio                              | 0.07 (0.06)        | 0.09 (0.06)        | 0.05 (0.05)        | 0.03 (0.04)        |                    | 0.06 (0.04)        |
| Clay_pct                              | 0.09 (0.06)        |                    |                    |                    |                    |                    |
| Soil_moisture                         | 0.01 (0.08)        | 0.07 (0.07)        |                    |                    |                    |                    |
| pH                                    | -0.18 (0.09)*      | -0.10 (0.06)       | -0.12 (0.06)+      |                    |                    | -0.07 (0.04)+      |
| Alpha_diversity                       | -0.03 (0.05)       | -0.01 (0.05)       | -0.02 (0.04)       | -0.02 (0.04)       | 0.00 (0.04)        | -0.04 (0.04)       |
| Total_Carbon_pct ×<br>DOM_conc        | -0.19 (0.09)+      | -0.14 (0.08)+      | -0.16 (0.07)*      | -0.14 (0.07)*      | -0.15 (0.07)*      | -0.13 (0.06)*      |
| Total_Carbon_pct ×<br>CN_ratio        | -0.08 (0.09)       | -0.02 (0.07)       | 0.02 (0.06)        | -0.05 (0.05)       |                    |                    |
| Total_Carbon_pct ×<br>Clay_pct        | 0.00 (0.12)        |                    |                    |                    |                    |                    |
| Total_Carbon_pct ×<br>Soil_moisture   | -0.13 (0.09)       | -0.07 (0.06)       |                    |                    |                    |                    |
| Total_Carbon_pct × pH                 | -0.12 (0.13)       | -0.15 (0.11)       | -0.02 (0.06)       |                    |                    |                    |
| Total_Carbon_pct ×<br>Alpha_diversity | 0.13 (0.08)        | 0.11 (0.07)        | 0.11 (0.05)*       | 0.10 (0.05)*       | 0.10 (0.05)*       | 0.11 (0.04)*       |
| DOM_conc × CN_ratio                   | -0.16 (0.16)       | 0.04 (0.12)        | 0.05 (0.12)        | 0.12 (0.12)        |                    |                    |
| DOM_conc × Clay_pct                   | 0.04 (0.13)        |                    |                    |                    |                    |                    |
| DOM_conc ×<br>Soil_moisture           | 0.08 (0.11)        | 0.00 (0.09)        |                    |                    |                    |                    |
| DOM_conc × pH                         | 0.06 (0.11)        | -0.02 (0.10)       | -0.02 (0.10)       |                    |                    |                    |
| DOM_conc ×<br>Alpha_diversity         | -0.24 (0.13)+      | -0.29<br>(0.10)**  | -0.31<br>(0.06)*** | -0.29<br>(0.06)*** | -0.27<br>(0.06)*** | -0.29<br>(0.05)*** |
| CN_ratio × Clay_pct                   | 0.13 (0.08)        |                    |                    |                    |                    |                    |
| CN_ratio × Soil_moisture              | 0.04 (0.07)        | 0.06 (0.06)        |                    |                    |                    |                    |
| CN_ratio × pH                         | 0.03 (0.08)        | 0.16 (0.05)**      | 0.14 (0.05)**      |                    |                    | 0.10 (0.04)**      |

|                                 |              |              |              |              |        |               |
|---------------------------------|--------------|--------------|--------------|--------------|--------|---------------|
| CN_ratio × Alpha_diversity      | 0.09 (0.07)  | 0.11 (0.06)+ | 0.10 (0.05)+ | 0.12 (0.05)* |        | 0.14 (0.04)** |
| Clay_pct × Soil_moisture        | -0.04 (0.13) |              |              |              |        |               |
| Clay_pct × pH                   | -0.16 (0.10) |              |              |              |        |               |
| Clay_pct × Alpha_diversity      | -0.07 (0.06) |              |              |              |        |               |
| Soil_moisture × pH              | 0.10 (0.09)  | 0.11 (0.08)  |              |              |        |               |
| Soil_moisture × Alpha_diversity | 0.00 (0.07)  | 0.03 (0.06)  |              |              |        |               |
| pH × Alpha_diversity            | -0.10 (0.10) | -0.05 (0.08) | -0.09 (0.07) |              |        |               |
|                                 |              |              |              |              |        |               |
| Num.Obs.                        | 56           | 56           | 56           | 56           | 56     | 56            |
| R2                              | 0.885        | 0.860        | 0.842        | 0.796        | 0.748  | <b>0.831</b>  |
| R2 Adj.                         | 0.765        | 0.774        | 0.783        | 0.751        | 0.717  | 0.793         |
| AIC                             | 27.0         | 23.7         | 18.6         | 22.7         | 26.8   | <b>12.4</b>   |
| BIC                             | 87.7         | 70.3         | 53.0         | 47.0         | 43.0   | 36.7          |
| Log.Lik.                        | 16.520       | 11.139       | 7.720        | 0.633        | -5.383 | 5.825         |

- Koch, B.P., Dittmar, T., 2006. From mass to structure: an aromaticity index for high-resolution mass data of natural organic matter. *Rapid Communications in Mass Spectrometry* 20, 926–932. doi:10.1002/rcm.2386
- LaRowe, D.E., Van Cappellen, P., 2011. Degradation of natural organic matter: A thermodynamic analysis. *Geochimica et Cosmochimica Acta* 75, 2030–2042. doi:10.1016/j.gca.2011.01.020